**PONTIFICIA UNIVERSIDAD CATÓLICA DE CHILE**
**Doctorado en Neurociencias**

Tesis Doctoral

# Cornifelin expression during *Xenopus laevis* metamorphosis and in response to spinal cord injury

Tesis presentada a la Pontificia Universidad Católica de Chile como parte de los requisitos para optar al grado de Doctor en Neurociencias

**Por**

**Sol Torruella González**

Director de Tesis: Dr. Juan Larraín Correa

Comisión de Tesis: Dra. Margarita Calvo
Dr. Pablo Henny
Dra. Ximena Sierralta

**Date 01/14/2022**

**PONTIFICIA UNIVERSIDAD CATÓLICA DE CHILE**
**Doctorado en Neurociencias**

El Comité de Tesis, constituido por los Profesores abajo firmantes, aprueba la Defensa Pública de la Tesis Doctoral titulada:

**CORNIFELIN EXPRESSION DURING *XENOPUS LAEVIS* METAMORPHOSIS AND IN RESPONSE TO SPINAL CORD INJURY**

**Aprobación Defensa:**

**SOL TORRUELLA GONZÁLEZ**

Calificándose el trabajo realizado, el manuscrito sometido y la defensa oral, con nota

6,7 (seis coma siete)

Director de Investigación y Doctorado
Escuela de Medicina
Pontificia Universidad Católica de Chile

Dr. Felipe Heusser
Decano
Facultad de Medicina
Pontificia Universidad Católica de Chile

Dra. Claudia Sáez
Sub-Directora
Dirección de Investigación y Doctorado
Escuela de Medicina
Pontificia Universidad Católica de Chile

Dr. Juan Larraín Correa
Director de Tesis
Facultad de Biología
Pontificia Universidad Católica de Chile

Dr. Francisco Aboitiz D.
Jefe Programa Doctorado en Neurociencias
Centro Interdisciplinario de Neurociencias
Facultad de Medicina
Pontificia Universidad Católica de Chile

Dr. Pablo Henny
Profesor Evaluador Interno
Facultad de Medicina
Pontificia Universidad Católica de Chile

Dra. Margarita Calvo
Profesor Evaluador Interno
Facultad de Biología
Pontificia Universidad Católica de Chile

Dra. Jimena Sierralta
Profesor Evaluador Externo
Facultad de Medicina
Universidad de Chile

**Santiago, 14 de enero 2022**

## Resumen

*Xenopus laevis* tiene la capacidad de regenerar luego de un daño en sus estadios larvales (NF-50), pero al término de la metamorfosis pierde esta capacidad (NF-66). En una secuenciación de ARN de alto rendimiento, se analizaron los transcritos de animales NF-50 y NF-66, 21 horas, 2 y 6 días luego del daño a la médula espinal por transección. Cornifelina fue uno de los transcritos más altamente expresados dos días después del daño en NF-66, lo que sugiere un rol luego del daño a la médula espinal. La expresión de cornifelina ha sido detectada previamente principalmente en epitelios escamosos estratificados como piel y mucosas, pero su expresión en estructuras del sistema nervioso central no ha sido descrita.

Aquí, usando técnicas histológicas, moleculares y bioquímicas, reportamos la expresión de cornifelina en la médula espinal, en la retina y en la córnea de *Xenopus laevis* durante la metamorfosis; evaluamos la reacción meníngea luego del daño por transección de la médula espinal y caracterizamos una línea transgénica para cornifelina.

La expresión de cornifelina fue detectada en la sustancia gris y meninges de la médula espinal de animales NF-50 y NF-66. La expresión en la sustancia gris disminuyó a lo largo de la metamorfosis. En retina, cornifelina fue detectada en la capa de células ganglionares, en las capas nucleares internas y externas y en el segmento externo en NF-50 y NF-66. Luego del daño a la médula espinal, la expresión de cornifelina fue regulada a la alta en animales NF-66. Además, encontramos que la expresión en meninges fue distinta luego del daño en NF-50 y NF-66. En NF-50, células positivas para cornifelina fueron encontradas cerrando el sitio de daño un día luego de la transección. En los siguientes días, fue encontrada delineando el tejido nervioso en reconexión. Por otro lado, en NF-66, células positivas para cornifelina fueron encontradas en las meninges y en la porción ventral de la médula a los seis días luego del daño y en el sitio de daño a los diez días.

Estos resultados sugieren que cornifelina participaría en la reacción meníngea luego del daño por transección a la médula espinal.

## Summary

*Xenopus laevis* can fully regenerate after an injury in their larval stages (NF-50) but loses it when metamorphosis is complete (NF-66). On a high-throughput RNA sequencing analysis, the transcripts from tadpoles (NF-50) and froglets (NF-66) after twenty-one hours, two and six days after spinal cord injury were analyzed. Cornifelin was one of the differentially expressed genes detected on the spinal cord from NF-66 animals two days after the injury, suggesting a role after spinal cord injury. Cornifelin expression has been found mainly on stratified squamous epithelia like epidermis and mucosa, but its expression on the spinal cord and other central nervous structures is not described.

Here, we used histological, molecular, and biochemical techniques to report the expression of cornifelin on the spinal cord, retina, and cornea of *Xenopus laevis* during metamorphosis; evaluate the meningeal reaction after spinal cord injury, and characterize a transgenic line for cnfn.

Our results detected cornifelin expression on the grey matter and meninges of the spinal cord from NF-50 to 66. The expression on the grey matter decreased during metamorphosis. On the retina, cornifelin was expressed in the ganglion cell layer, the inner and outer nuclear layer, and the outer segment from NF-50 to 66. After spinal cord injury, the expression of cornifelin was upregulated at NF-66. In addition, cornifelin expression on the meninges was distinct between NF-50 and NF-66. In regenerative animals, cornifelin positive cells from the meninges were found closing the stumps one day after the injury. On the following days were found delineating the spinal cord as the tissue recovered its continuity. On the other side, on non-regenerative animals, positive cells from the meninges were found distributed on the ventral side six days after the injury and the injury gap ten days after the injury.

These results suggest that cornifelin participates in the meningeal reaction after spinal cord injury.

*A mis padres*

*Y a mis abuelos Sara y Guillermo*

## Acknowledgments

I would like to thank my tutor, professor Juan Larraín Correa, for accepting me into his laboratory and his continuous support during my Ph.D. work. I got the opportunity to work with *Xenopus laevis*, a beautiful model, and I started to become a scientist while studying cornifelin. Thank you for the opportunity, the motivation, and the patience.

I also want to thank to Dra. Paula Slater for the support and the motivation on the last part of this work. Thank you for the perspective, the words of encouragement, and the coffee.

Thanks to the "JAL LAB" members for their comments and help during my experimental work.

Thanks to my thesis committee: Dra. Margarita Calvo, Dr. Pablo Henny, and Dra. Jimena Sierralta, for enriching this work with their comments and discussion.

But above all, I would like to express my gratitude to my parents because even when they do not understand why I chose this path, they have let me explore it and pursue a career in science with everything involved.

# Table of Content

# TABLE OF FIGURES

**Abbreviations list**

*In alphabetical order*

BrdU: Bromodesoxiuridina

Cnfn: Cornifelin

CNS: Central nervous system

CSPGs: Chondroitin sulfate proteoglycans

DEG: differentially expressed genes

DEPC: Diethyl pyrocarbonate

ECM: Extracellular matrix

GFAP: Glial fibrillary acidic protein

hCG: Human chorionic gonadotropin

mRNA: Messenger ribonucleic acid

MS222: Ethyl 3-aminobenzoate methanosulfonate

ON: Overnight

PBS: Phosphate buffer saline

PFA: Paraformaldehyde

PNS: Peripheral nervous system

RIPA: Radioimmunoprecipitation assay buffer

RNA-seq: RNA sequencing analysis

RT: Room temperature

SCI: Spinal cord injury

SC-seq: Single cell sequencing analysis

TEA: Triethanolamine

# 1.INTRODUCTION

## 1.1 Spinal cord injury in regenerative and non-regenerative organisms:

Yearly, between 250,000 and 500,000 people suffer a spinal cord injury (SCI). This occurs mainly because of falls, car accidents, sports injuries, violence, or other events such as infectious diseases or tumors (World Health Organization, 2013). The damage produces the loss of the sensitive and motor function below the injury site.

Following SCI, a secondary wave of damage compromises the tissue surrounding the lesion site. This secondary damage is classified in acute, sub-acute, and chronic phases. The acute phase starts right after the lesion and consists of vascular injury, ischemia, and hypoxia. The sub-acute phase comprises death of oligodendrocytes and neurons, demyelination, Wallerian degeneration, axonal dieback, extracellular matrix remodeling, and glial scar formation. The chronic phase encompass the cystic cavity formation and the maturation of the scar (Alizadeh, Dyck, & Karimi-abdolrezaee, 2019). In mammals, these processes lead to the loss of function as axons are unable to regenerate and reconnect.

This inability of axons to regenerate is explained by to two main factors: the intrinsic and extrinsic responses of the tissues involved. The intrinsic factors hypothesis is related to the absence of neuronal inner mechanisms that allow growth of the axons from the damaged neurons. For the growth of the axons, a growth cone must form at the edge of the damaged axon, but in the central nervous system (CNS), a retracting bulb is formed instead. This structure presents a swollen morphology, and their cytoskeletal components such as microtubules and actin are disorganized, impeding their assembly and stabilization for the extension of the axon

after the injury. In addition, the gene expression after the injury promotes this unfavorable response (He & Jin, 2016).

On the other hand, extrinsic factors refer to the presence of a non-permissive environment in the CNS. This hypothesis is based on the classic experiment from Aguayo and collaborators (Duncan, 1981), which demonstrated that CNS axons are able to regenerate through an implant of nerve coming from the peripheral nervous system (PNS). But, when they inverted the conditions, PNS axons were unable to grow on nerves from the CNS, suggesting that the CNS environment impedes the regeneration of damaged axons.

The scar is another extrinsic factor that blocks the elongation of the axons after an injury. This scar is composed of two different cellular responses. On the epicenter of the lesion, a fibrotic scar consisting of meningeal cells that proliferate and migrate to the injury site is formed (Decimo, 2011). In addition, covering but not mixing with, it is the glial scar. This lining scar is formed by reactive astrocytes that proliferate, arrive at the lesion site, enclose sprouting axons (Frisén J, 1995), accumulate glial fibrillary acidic protein (GFAP), and release extracellular matrix like chondroitin sulfate proteoglycans (CSPGs) (Silver & Miller, 2004; Silver, Schwab, & Popovich, 2015) to enclose the damage and prevent its expansion (Pekny et al., 2016; Sabelström et al., 2013). But this deposition is also an inhibitory signal for the growth of axons (Bradbury & Carter, 2011; Yuan & He, 2013). Although recent studies show that the glial scar could be a permissive substrate for the regrowth of ascending sensory axons (Anderson et al., 2016), all the other players like fibroblasts, CSPGs and inflammatory mediators would play a negative role on the regrowth of them.

In contrast, regenerative animals develop a different cellular response. In zebrafish and salamanders, two organisms that can regenerate the spinal cord during their whole lifespan, the glial cells from the ependymal layer of the central canal have neural progenitor characteristics. After an injury, they proliferate and differentiate into neurons. They also provide a permissive environment for axon regeneration (Becker, Becker, & Hugnot, 2018). A subpopulation of ependymal cells positive to SOX2 reacts to injury, increasing its expression and proliferating. In zebrafish, it seems to be the initiator of the proliferation because its deletion reduces the proliferation rate (Ogai et al., 2014). This also happens after this deletion in axolotl, affecting the regeneration of the spinal cord due to a decrease in proliferation (Fei et al., 2014). *SOX11* is also an active player in zebrafish in response to the injury, promoting the expression of *ascl1* and *nestin*, proneural and stem cells markers, respectively (Guo et al., 2011).

### 1.2.- *Role of meningeal cells in spinal cord regeneration*

Meningeal cells also react to the injury, but contrary to what happens in non-regenerative animals, in regenerative ones like axolotl they form a physical conduit for axon regeneration. These cells guided the growing axons to reach the injured site after two weeks and wrapped around them to give them a substrate to travel in. In this model a chronic barrier on the injury site is not formed, and extracellular matrix (ECM) proteins are not inhibitory (Zukor, 2011). The formation of this bridge in zebrafish depends on *ctgf*. In absence of *ctgf*, the spinal cord regeneration is affected (Mokalled et al., 2016). Furthermore, in an in vitro model of spinal cord development, attractive and repulsive cues from the meninges guided sensory and motor axons

to their final destination (Suter et al., 2017), suggesting a role on axon pathfinding that can be recapitulated after the injury in regenerative animals.

The evidence suggests that meningeal cells would have a dual role in regeneration, being detrimental in mammals and required for proper regeneration in capable model organisms.

Meninges are formed by three layers, the dura, arachnoid, and pia mater, these latter two are organized together so they are called leptomeninges. Meninges surround the neural tissue, protecting the brain and the spinal cord from external cues (Russi AE, 2015).

The dura is a thick membrane highly vascularized, in close relation with the vertebrae and are composed of fibroblast, collagen, and elastic fibers. The arachnoid layer consists of flattened cells surrounded by collagen and fibrous tissue, organized in a stratified manner with an inner barrier and a external one expressing tight junctions as claudin11 and e-cadherin (Derk et al., 2021). In amphibians, there are approximately 14 layers joint by desmosomes and cytokeratins (Achtstatter, 1989), suggesting an epithelial-like cytoskeleton.. The innermost membrane, the pia, is a flat layer of one cell of thickness that is continuous and joined together by desmosomes and gap junctions. It contains connective tissue, mainly collagen(Morse & Low, 1972). Right under the pial layer, the basal membrane is formed by collagen, fibroblast, and macrophages. These components separate the neural tissue from the meninges (Morse & Low, 1972; Nicholas & Roy, 1988; Reina MA, 2004).

## 1.3.- *Spinal cord regeneration in Xenopus laevis and cornifelin*

We use *Xenopus laevis* as a model to study regeneration. *Xenopus* has the capability of fully restore its spinal cord after an injury in its larval stages (NF 50-54, tadpoles, R-stage), but when metamorphosis is complete (NF 66, froglets, NR-stage), they lose it (Gaete et al., 2012). Other advantages of this model are their external embryonic development, a high number of individuals in a single mate event, easy handling, small size in early stages, a sequenced genome, and the possibility of making transgenic animals.

Previously, our laboratory was interested in identifying the differences in response to spinal cord transection in the R-stage and NR-stage of *Xenopus laevis*. To achieve this, a high-throughput RNA sequencing analysis was performed. The spinal cords from the R and NR-stages were isolated at 21 hours, 2 and 6 days after transection injury and were compared with sham-operated animals at the same temporal points post-surgery. This experiment detected an extensive list of differentially expressed transcripts in R and NR-stages (Lee-liu et al., 2014). Neurogenesis-related transcripts like *neurod4* and *ascl1* were upregulated in R-stage, while in NR-stage these genes were down-regulated. Moreover, SOX factors, associated with neural progenitors, *soxd* and *sox21*, were also upregulated in R-stage.

Interestingly, NR-stage has a delay in the upregulation of these genes, which may offer an opportunity window for regeneration, as the activation of SOX2/3+ cells is crucial to the functional recovery of tadpoles and happens on day 6 (Muñoz et al., 2015). The BrdU incorporation is also delayed comparing these two stages. In NR-stage, this happens just on day 6.

One of the three most differentially expressed genes (DEG) found in the RNA-seq was cornifelin (*cnfn*). This gene was highly upregulated in the three temporal points analyzed in NR-stage, while their levels were unchanged in the R-stage (Lee-liu et al., 2014). The contrasting behavior observed in cornifelin mRNA suggests it has a role in regeneration.

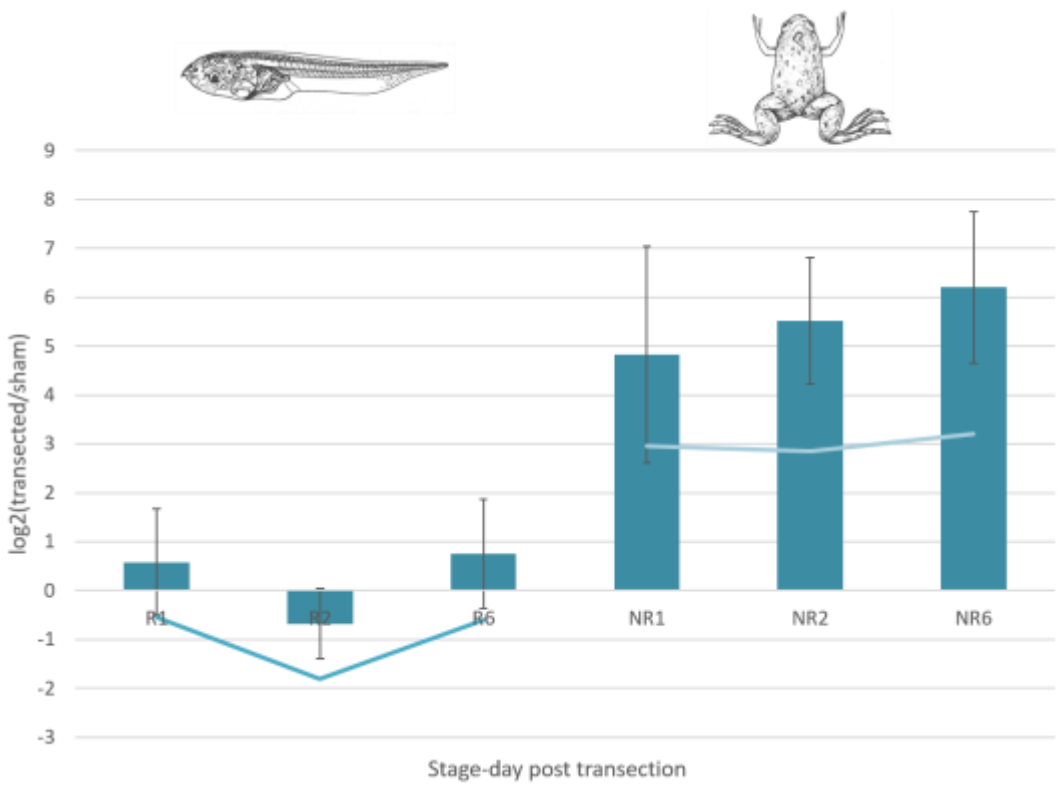


Figure 1. Cnfn mRNA levels after spinal cord injury in Xenopus laevis. Cnfn levels detected by RT-qPCR were normalized against eef1a1 in both transected and sham samples after 21 hours, 2 and 6 days post transection injury in R and NR-stage. Log2 from the fold change of the ratio transected/sham was graphed. Data from: Lee-Liu D, 2014, not published.

Cnfn is a member of the Plac8 protein family. These proteins share a cysteine-rich domain and are located on the inner side of the plasma membrane. Among the functions described for members of the family are the control of cell number, fruit size, and heavy metal resistance in

vegetal cells (Song WY, 2011); apoptosis, proliferation, differentiation, epithelial to mesenchymal transition, and autophagy in animal cells (Cabreira-Cagliari et al., 2018).

Although cnfn expression is low in uninjured contexts, cnfn expression has been found in fetal skin and mucosa from the uterus, cervix mouth, pharynx, and esophagus (Michibata et al., 2004; Wagner et al., 2019), all stratified squamous epitheliums. The human protein atlas also showed cnfn on other stratified squamous epitheliums such as the salivary gland, tongue, tonsil, airways, testis, prostate, vaginal mucosa, breast, lymphoid tissue, and urinary bladder (Human Protein Atlas available from http://www.proteinatlas.org, v20.1(Uhlen M, 2010)). Recently, cnfn was detected on dermal fibroblast from newborn mice (Wang et al., 2021).

Our understanding about the function of cnfn is very limited. Overall, cnfn expression increases after an injury. In inflammatory skin diseases like psoriasis, dermatitis, and eczema, cnfn is overexpressed and located from the granular to the horny cell layer of the epidermis (Michibata et al., 2004). In addition, in an *in vitro* model of human corneal epithelium, cnfn was upregulated after exposition to irritants such as triton x-100 (Choi et al., 2014).

In mice, five cysteine residues are substrates of the palmitoyl-acyl transferase enzyme Zdhhc-13, with two positions required for the proper stability and expression of cnfn. Furthermore, the absence of post-translational palmitoylation results in the detachment of both the skin and hair cells under mechanic stress (Liu et al., 2015). More recently, Wagner et al. (Wagner et al., 2019), found that cnfn is also necessary for the attachment of keratinocytes from oral mucosa and epidermis, as cnfn knock-down results in alterations in the morphology and number of corneodesmosomes on the cornified layer with the subsequent detachment of the cells.

Desmoglein 1 expression is also affected by the absence of cnfn, suggesting that cnfn is implied in the adhesion process.

The overexpression of cnfn in mice keratinocytes, results in the upregulation of involucrin, a marker of differentiation, and the downregulation of loricrin (Michibata H et al., 2004), suggesting that the increase of cnfn resembles the injured context seen in psoriasis.

Cnfn is downregulated if the transcription factor SIX1, which is present in the development of the cranial sensory placodes, is knock-down from *Xenopus* embryos. This may indicate a role in the sensory placode development (Yan et al., 2015). Besides, cnfn is also downregulated if IFN$\alpha$ receptor 1 (IFNAR1) is knocked-out in mice (Grine L , 2015), which suggests that cnfn could be a downstream player of this pathway.

Furthermore, many gene expression profile studies as microarrays, RNA-seq, and SC-seq analyses detect cnfn in their samples in several and related topics like epithelium damage, inflammation, cancer, baldness, and tissue regeneration. However, these works do not deepen over the function of cnfn.

In summary, cnfn is present in stratified epithelia that shed frequently like epidermis, mucosa, and cornea, and react to injury, increasing its expression. On the other hand, cnfn directly affect the expression and function of corneodesmosomes, resulting in the detachment of keratinocytes from oral mucosa and epidermis. In the central nervous system, leptomeningeal layers also express desmosomes as intercellular junctions. After the injury, these layers migrate to the injury site to re-establish the lining of the nervous tissue. In this work, I propose that cnfn is expressed

in the spinal cord, cornea, and leptomeningeal cells and would have a role in the regeneration process of the spinal cord of *Xenopus laevis*.

## 2. HYPOTHESIS

"Cnfn is expressed in the spinal cord, cornea, and the leptomeninges, and its expression levels are regulated after spinal cord transection injury in *Xenopus laevis*."

General Aim

Determine the expression of cnfn during metamorphosis in the spinal cord and the eye, and in response to spinal cord injury.

Specific Aims

1) Characterize the expression of cnfn during metamorphosis in the spinal cord and the eye, and in the spinal cord and the leptomeninges in basal and injured conditions in regenerative and non-regenerative stages of *Xenopus laevis*.
2) Study the response of the meninges to spinal cord injury in R and NR-stage of *Xenopus laevis*.
3) Characterizate a cnfn trasngenic line.

# 3. MATERIALS AND METHODS

## *3.1 Growth of Xenopus laevis tadpoles and froglets*

All animal procedures were approved by the Committee on Bioethics and Biosafety from the Faculty of Biological Sciences, Pontificia Universidad Católica de Chile, n°170630005.

Animals were obtained by natural mating induced by human chorionic gonadotropin (hCG) in adults *Xenopus*. Animals were raised until they reach NF-50 for the regenerative stage (two weeks, R-stage) and NF-66 for the non-regenerative stage (two months, NR-stage) according to the morphological descriptions done by Nieuwkoop and Faber.

## *3.2 Spinal cord transection*

Animals were anesthetized in a petri dish with 0,02% of ethyl 3-aminobenzoate methanosulfonate (MS222) dissolved in 0,1x Barth buffer before surgery. The surgeries were made as described previously (Edwards-faret et al., 2017). Briefly, in R-stage, the transection surgery consists of a clean cut with iridectomy scissors that reach the skin, muscle, and spinal cord. The sham surgery consists in a clean cut that reach the skin and muscle and leaves the spinal cord intact. In NR-stage, anesthetized froglets were put on the top of a petri dish with gauze. The dorsal skin was longitudinally opened with the tip of a needle, and the muscle was cut to reach the vertebrae. The vertebrae, between the 5th and 6th was removed with the tips of the forceps, and the neural tissue exposed cut transversely with the scissors. Sham animals were

submitted to the same procedure but this stopped at laminectomy. To close the wound, the separated tissues, muscle, and skin were closed together at the line of the injury with the forceps. The animals were then maintained in tanks with Barth buffer 0,1x supplemented with antibiotics. Tanks had aeration, and the buffer supplemented with antibiotics were change any other day until the end of the experiment. We fed the animals the days that do not correspond to this changes to lessen startle responses.

### *3.3 RT-qPCR*

The RT-qPCR were performed accordingly with previous works (Lee-Liu et al., 2014). Total RNA was extracted with RNeasy Mini kit, quantified by a spectrophotometer, and 300 ng of each sample was used for synthesizing the cDNA using the M-MLV reverse transcriptase (Promega) at 42°C for 1 hour and 30 minutes. The RT-qPCR assays were performed using Maxima SYBR Green (Thermo Scientific). The relative expression ratio was calculated using the housekeeping gene *eef1a1*.

The primers sequence used for cnfn were:

Fw: GTTCGGCTCTATTCTTGCC

Rv: CCATTTGGCAGAGAGCAC

Fifteen animals were used for NF-50, ten forNF-54 stages, eight for NF-56 and NF-58, and three for NF-62 and 66 stages for each replicate of the RT-qPCR assay (three biological replicates).

*3.4 in situ hybridization*

We followed the protocol developed by LADE laboratory, Universidad de Concepción (Aldea et al., 2013.). A brief description of this protocol is described below.

R-stage animals were fixed in 4% paraformaldehyde (PFA) in phosphate buffer saline (PBS) 1x overnight (ON) at 4°C. The tissues were then dehydrated with an ethanol gradient ranging from 50% to 100% in diethyl pyrocarbonate (DEPC) treated water, 5 minutes each point. The last change was made for 20 minutes and then this solution was replaced with ethanol 100% and stored at -20°C until use.

Ethanol 100% was replaced with two changes of Xylene and gently shake the samples for 15 minutes. We next replaced with 50:50 solution of Xylene/Paraffin and incubated at 60°C for 15 minutes in a digital dry bath. Subsequently, this solution was replaced with 100% paraffin for 1 hour at 60°C. This step was repeated three times. After this, we moved the sample to a peel-away paraffin block with melt paraffin, in the desired position and leave it ON at 4°C. Paraffin embedding animals in R-stage were cut at 7 um thickness with a microtome.

Slides were treated with Xylene to remove the paraffin, and rehydrated in an ethanol gradient ranging from ethanol 100% to 25% ending with two changes of PBS 1X. Slides were left for 5 minutes in each solution. We post-fixed in PFA 4% for 20 minutes at room temperature. Next, we permeabilizated the slides in 0.1% PBS-Tween twice for 5 minutes. The sections were then incubated in proteinase K (10 ug/mL) in PBS 1x for 10 minutes at 37°C and post-

fixed afterwards in PFA 4% for 20 minutes at room temperature (RT). After two washes with 0.1% PBS-Tween, we acetylated the slides with Trietanolamine 0.1M, pH=7-8 and 0.25% acetic anhydride for 5 minutes at RT, to remove electric charges on the slide, and to avoid background probe binding on the tissue. The pre-hybridization was made in a humid chamber for 3 hours at 60°C. The buffer recipe can be found in the link presented above. For hybridization, we first denature the probes, used at a concentration of 100 ng in 150 uL of hybridization buffer, and heated them at 80°C for 5 minutes, then quickly chill them on ice for 5 minutes. We incubated the slides with the denatured probes at 60°C ON in a humid chamber, protected with a coverslip to avoid probe evaporation.

In the second day, we washed the slides in SSC 2x-0.1% CHAPS/50% formamide for 30 minutes at 60°C to lowered the hybridization temperature. Next, we washed the slides in TNE buffer with RNAse at 37°C to eliminate the excess probe that did not bound to the tissue. We blocked the tissue samples with goat serum 20% in Buffer 1 (1M Tris pH 7.5, NaCl 3M) for 1 hour at RT. Followed with the incubation of anti-DIG-AP 1:2000 in Buffer 1/20% goat serum ON at 4°C in a humidity chamber.

During the third day we prepared the samples for the chromogen reaction. We washed twice the slides in alkaline phosphatase buffer pH 9.5 for 5 minutes at RT. Next, the chromogen solution (NBT/BCIP) was placed on the slides and incubated in a humid chamber at 4°C for 19 hours. The reaction was stopped with PBS 1x.

For probe preparation we used a plasmid obtained comercially (IMAGE 6316571). The sense and antisense probes were synthetized in the laboratory, and the labeling was done with digoxigenin.

## 3.5 *Western blot*

### *3.5.1 Antibody preparation*

A specific peptide for *Xenopus leavis* cnfn was made. We defined the peptide sequence used for rabbit immunization comparing cnfn.1.L ad cnfn.1.S (homologues a and b, respectively). They shared 91% of homology, and it was not possible to found a portion that would allow us to discriminate one protein from the other. Besides, the cnfn sequence has 15 cysteine residues, which may form disulfide bonds and secondary structures, reducing the alternatives to choose a proper peptide for immunization. We chose the sequence -CKK-Ahx-VQGYMTSNSSQWNSDVF-amide for the generation of the peptide (Figure 5). This sequence is located closest to the amino portion of the protein and does not have any cysteine residue. The anti-rabbit polyclonal antibody was made by AntibodyBcn and purified by affinity.

### *3.5.2 Homogenization of cnfn*

Tissue samples were first homogenized with RIPA (radioimmunoprecipitation assay buffer) but it was not sufficient to detect a band in western blot. For this reason, we tried three different buffers to improve cnfn solubilization from the tissues: buffer SDS-PAGE 1x (diluted from 5x standard stock that consists of 10% SDS, 1M Tris pH 6.8, glicerol, ditiotreitol and a pinch of bromophenol blue); Triton x-100 1x, and urea 8M. We treated each sample with the buffer supplemented with protease inhibitors (benzamide 1uM; leupeptin 5 ug/ml; Na3VO4 200 um; sodium pyrophospahte 200 uM and phenylmethylsulfonyl fluoride 200 uM). Fifteen animals for

NF-50, tenfor NF-54 stage, eight for NF-56 and 58 stage and three for NF-62 and NF-66 were used for the protein assays. We use 100 uL of the lysis buffer to homogenizate NF-50 and NF-54; 150 uL to homogenizate NF-56 and NF-58; and 200 uL to homogenizate NF-62 and NF-66.

- RIPA homogenization: The homogenization was carried out on ice with a plastic homogenizer. After the tissue was no longer visible in the tube, lysates were centrifuged at 13000 rpm for 5 minutes at 4℃. The supernatant was rescued and stored at -20℃ until use. The samples were then quantified with the BCA protein assay kit.
- SDS-PAGE 1x homogenization: The samples were left with the buffer supplemented with proteinase inhibitors, for approximately 10 minutes before the homogenization. Next, the tissue was lysate on ice with a plastic homogenizer, until it was no longer visible found in the tube. The samples were centrifuged at 12000 rpm for 10 minutes at 4℃. The supernatant was rescued and stored at 20℃ until use. As the SDS-PAGE loading buffer is no compatible with the BCA quantification assay, we load the samples by volume. To do this, after thawing the protein samples on ice, we vortexed each tube briefly and spin every tube for 30 seconds to recover all the liquid that may got on the walls and top of the tube. Then, we took 10 uL of each sample after three up-and-down with the pipette.

We load the homogenizated samples, which represent 1.5 spinal cords approximately. For NF-54, we load 1 spinal cord approximately. For NF-56 and 58, we used 8 spinal cord in 150 ul of lysis buffer, thus 0.53 spinal cord approximately were loaded. For NF-62 and 66 we isolated 3 spinal cords in 200 ul of buffer, which represent 0.21 spinal cord loaded approximately. It is

worth to mention that the height and the weight of the animal increase through metamorphosis, this is the reason why we use less samples per animal as they grow.

- Urea 8M homogenization: The protein samples were homogenized on ice with a plastic homogenizator until the tissue was no longer visible on the tube. The samples were incubated for 1 hour with soft movement at RT and then the lysates were centrifuged at 12000 rpm for 10 minutes at 4°C.
- Triton x-100: This protocol was developed as described by Tsarouchas TM et al.,2018. The tissues were homogenized in 1% triton x-100 in PBS 1x with proteinase inhibitors; using a plastic homogenizator. The samples were left at 4°C for 1 hour and then centrifuged at 12000 rpm at 4°C for 20 minutes. The samples were then quantified with the BCA protein assay kit.

We tried two different incubations before loading the samples in the electrophoresis gel: standard load with SDS-PAGE 5x and urea 8M (to a final concentration of 2x from stock).

- SDS-PAGE incubation: The proteins were boiled for 5 minutes at 95°C in a digital dry bath. After this, the samples were spin, ice cooled for 5 minutes, and loaded in the 15% SDS-PAGE gel.
- Urea 2x incubation: Lysates were heated at 37°C for 1 hour before loading the samples in the 15% SDS-PAGE gel.

After electrophoresis, proteins were transferred to a PDVF membrane for 1 hour and 30 minutes at 350 mA.

The antibodies used in this work were anti-rabbit cnfn at a 1:5000 dilution and anti-mouse a-tubulin at a 1:40000 dilution.

### *3.6 Immunohistochemistry*

Fixation of tissues was made by immersion of the R-stage animal (NF-50) or transcardial perfusion with 4% PFA-PBS 1x in NR-stage animals (NF- 66). For NR-stage animals, an extra step was done with the decalcification of the vertebrae, incubating the fixed animals in 0.5M EDTA in PBS 1x for 24 hours at 4°C with movement.

Ten µm paraffinized slices were made with the microtome and mounted with water at 55°C in charged slides. The slides were then left in the oven for 1 hour at 60°C to dry. Next, the slides were submitted to a deparaffinization process with Xylol and to a rehydration process in ethanol from 100% to 50%. Afterwards, the tissue was immersed in a coupling jar with EDTA 1mM/tween 20 0.05%, pH=8 at 95°C in a water bath for 40 minutes to unmask epitopes. In transverse sections, lesser times results in a poorly detection of cnfn and higher times compromises the integrity of the tissue. After this, the protocol for immunohistochemistry followed a previously described one (Méndez-Olivos, 2017) with minor modifications. The blocking of the peroxidase activity was made with 0.3% $H_20_2$ and developed for fifteen minutes, followed by a permeabilization step with 0.2% triton x-100 in PBS 1x (PBST) for ten minutes. The blocking step was made with 10% goat serum in PBST for thirty minutes. The incubation with the primary antibody (cnfn 1:100) was made for at least 18 hours at 4°C in blocking

solution. The secondary anti-rabbit-HRP, 1:500 was left 2 hours at RT. The detection step was made with DAB peroxidase HRP kit (Vector laboratory SK4100) for five minutes at RT for NF-50 and NF-66 tissue when we compared the expression on metamorphosis experiments. The reaction was developed for 10 minutes in NF-66 in injured experiments

### *3.7 Immunofluorescence*

Eyes from R-stage, were isolated and used as a positive control for the immunodetection of cnfn. The tissues were fixed in 4% PFA in PBS 1x. The samples were treated with NaBH4 at 1mg/ml diluted in a $Ca^{+2}$ and $Mg^{+2}$ free buffer for 15 minutes to reduce the autofluorescence of the tissue, and then washed in this buffer for ten minutes. The samples followed a standard protocol described previously (Gaete et al., 2012). First were permeabilized in 0.2% PBST and blocked with goat serum at 10% in the same solution. The incubation with the primary antibody (cnfn, 1:100 dilution) was done overnight at 4°C in PBSt. The secondary Alexa antibody is incubated at 1:500 dilution for two hours at RT in PBSt, and then the slides were incubated with Hoechst solution (1:40000) for five minutes, and mounted with Vectashield (H-1000-NB).

### *3.8 Masson stain*

The samples were fixed in PFA 4% and 10 um cryosections were made. The slides were kept for 1 hour in Bouin solution at 65°C. The nucleus was then stained with fresh iron hematoxylin for 10 minutes and then washed with running water for 10 minutes. The slides were then treated with acid fucsin for 30 seconds and with aniline blue for collagen stain.

### *3.9 Hematoxylin & Eosin*

The nucleus were stain with gill hematoxylin for one minute and the washed with running water for 10 minutes. After dehydration with an ethanol gradient ranging from 50 to 90%, the slides were stain with eosin for 30 seconds and completely dehydrated with two washes of ethanol 100% for 5 minutes. The slides cleared with xylol and mounted with Entellan.

### *3.10 Transgenic line to cnfn: Animal groups*

Transgenic animals have the crystalline red under fluorescence laser. These animals overexpress cnfn after heat shock treatment. Animals were selected according to the color of their eyes and heat shock treatment and divided into 4 groups:

- Black eyes (BE): Animals that did not carry the transgene and did not were submitted to heat shocks protocols.
- Black eyes + Heat Shock (BE+HS): Animals that did not carry the transgene and were submitted to heat shock protocols.
- Red eyes (RE): Animals that carry the transgene and did not were submitted to heat shocks protocols.
- Red eyes + Heat shock (RE+HS): Animals that carry the transgene and were submitted to heat shocks protocols.

### *3.11 Heat shock protocol*

Tadpoles were incubated in 0.1x Barth buffer at 34°C for 30 minutes. This protocol was performed one day after injury and repeated any other day until day eleven, performing a total of 6 heat shocks.

### *3.12 Qualitative analysis of tadpole responses after spinal cord injury*

The head skin of the tadpole was carefully touched with a Pasteur pipette and the evasive response if any was annotated and analyzed between the groups. The responses fall in three categories: a) parapeglia, characterized by a weak movement of the head but no response below the injury site; b) Circular swimming, characterized by the turn of the animals in 360°; c) Coordinated swimming, consists on the total recovery of the movement characterized by an undulatory behavior of the whole tail (Gaete et al., 2012).

### *3.13 Quantitative analysis of tadpoles swimming behavior after spinal cord injury*

After 5 minutes of habituation on a petri dish with 0.1x Barth buffer, we recorded the animal swimming with the software AnyMaze. The total distances swam were quantified for each group.

### *3.14 Sequencing of the transgene in Red eyes animals*

The genomic DNA extracted from RE animals was sequenced by the Sequencing system facility of the Pontificia Universidad Católica de Chile with the promoter for Sp6 and T7. The sequences were analyzed and compared with the original designed construct in SnapGene.

# 4. RESULTS

## 4.1.- *Cnfn expression during Xenopus laevis metamorphosis*

### 4.1.1.- *Expression in the spinal cord*

#### *4.1.1.1.- RT-qPCR analysis*

The expression of cnfn in the spinal cord has not been described. For this reason, we decided to investigate its expression levels during different metamorphic stages (NF-50, 54, 6, 58, 62 and 66). To address this, we performed RT-qPCR analysis on the isolated spinal cord from each stage. Cnfn mRNA levels were normalized to the housekeeping gene *eef1a1*. The mRNA levels decreased from NF-50 to NF-66 (Figure 2A). When we compared NF-50 levels (the temporal point with the highest levels) to NF-66 (the temporal point with the lowest levels), we found a reduction of almost 80% (Figure 2A, inset), and this difference was statistically significant. Another observation that came to our attention was the wide variability of the levels observed between different biological replicates (Figure 2B), that were more pronounced in regenerative stages (NF 50 and 54).

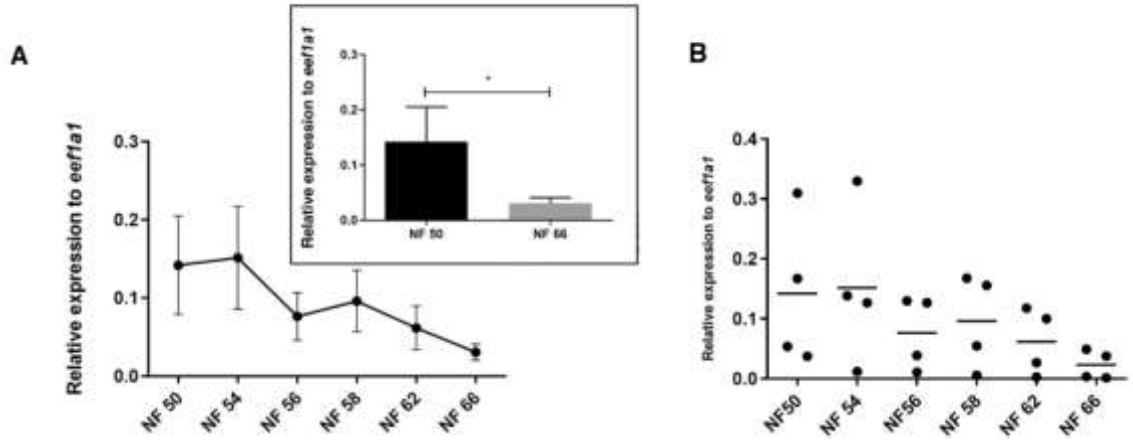


Figure 2**.** *Cnfn* RNA levels in the spinal cord during *Xenopus laevis* metamorphosis*.* A*) Cnfn m*RNA levels detected by RT-qPCR were normalized against *eef1a1* (average ± SEM, n=4 for all the stages studied). The inset show the comparison of the levels of cnfn between NF 50 and 66. A double-tail t-test between these stages found a statistical difference (p=0.0138). B) Shows the results for the four biological replicates as a dot plot.

*4.1.1.2.- in situ hybridization*

We performed in situ hybridization to confirm the expression of cnfn in the spinal cord and know its mRNA localization. The protocol commonly used in our laboratory for early embryonic stages was not helpful for the later stages studied in this thesis. For that reason, I learned and set up the protocol used by the LADE laboratory in Universidad de Concepción (Aldea et al., 20013). Briefly, the differences with our protocol were the following: the new protocol use 7 µm paraffin-embedded sections instead of 10 µm cryosections. All material used is incubated with NaOH 0.5M the night before starting the protocol to eliminate RNases. It uses Triethanolamine (TEA) at 0.1M (pH=7-8, with 0.25% acetic anhydride) to reduce the background. TEA diminishes the non-specific union of the probe to the slides and the tissue samples by acetylation of polar and charged groups. This new protocol also uses citrate buffer instead of phosphate buffer for washing steps and the elaboration of the hybridization buffer. All these changes in the protocol were adopted for the study of cnfn expression.

We prepared the sense and antisense probes from commercial plasmid for cnfn (IMAGE 6316571, for cnfn.1.L gene). Probes for col2a1 and Sox2, used as positive controls, were kindly facilitated by the LADE laboratory. The four probes used for stage 50 were used at 1:150 dilution (100 ng of probe approximately, quantified with Qubit) in serial longitudinal sections of the spinal cord.


Figure 3. Sox2 RNA expression in the spinal cord of regenerative animals. *In situ hybridization* in longitudinal sections from NF-50 animals. The antisense probe results are shown. Insets show magnifications of boxed areas: a) thoracic magnification from the spinal cord. b) Nerve root.

The Sox2 antisense probe hybridized in the ependymal cells of the central canal as expected from literature (Gaete et al., 2012, Muñoz et al., 2015) (Figure 3). Sox2 was also found in the cells of the grey matter and nerve roots, with a constant expression ranging from rostral to caudal.

The Col2a1 antisense probe detected an intense expression in the chondrocytes of the vertebral processes as expected (Figure 4) and was also found in nerve roots, in the *cauda* equina, and cells from the grey matter, with a diffuse expression toward lateral regions.

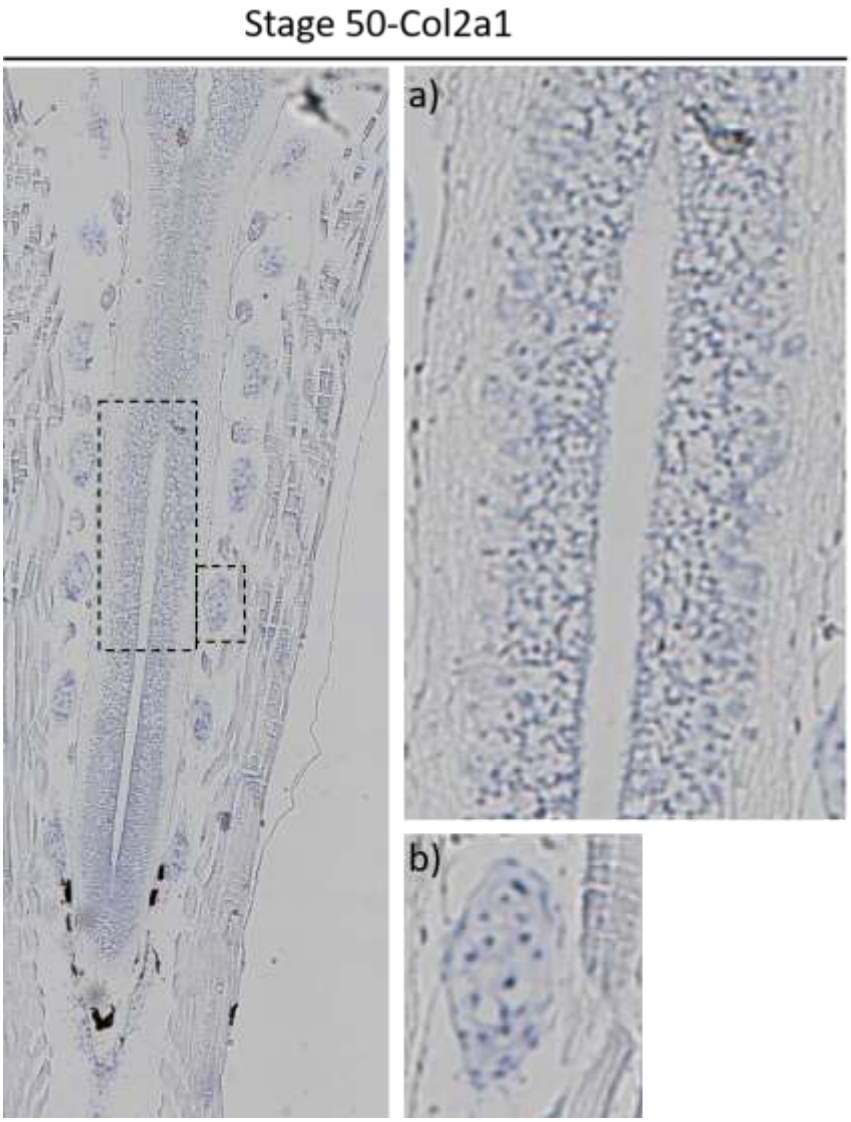


Figure 4. Col2a1 RNA expression in the spinal cord of regenerative animals. *In situ hybridization* in longitudinal sections from NF-50 animals. The antisense probe results are shown. Insets show magnifications of boxed areas: a) thoracic magnification from the spinal cord. b) Chondrocytes from the vertebral processes.

The antisense probe for cnfn hybridized in the NF-50 spinal cord (Figure 5). From external to internal structures, cnfn expression was detected in the pial layer of meninges covering the neural tissue (Figure 5A), in scarce neurons found on the white matter. Cnfn was also detected in neurons in the medial and lateral regions of the grey matter (Figure 5B), and in the ependymal cells from the central canal (Figure 5C). The cnfn sense probe (negative control) did not hybridize in the tissue tested (Figure 5D).

In the pial layer, the intensity of cnfn expression was constant from rostral to caudal regions. In the grey matter, we found rounded and polygonal cell bodies of similar sizes. These neurons showed different patterns of expression.

The positive labeling observed in the ependymal cells from the central canal (Figure 5C) had a stronger intensity in the basal surface of these cells, which tend to diffuse through the elongated nucleus, then increased again in the apical surface.

This protocol detected a positive signal in the spinal cord for the three genes tested. Each gene expression had different intensities in the cells from the grey matter, where Sox2 positive cells were most intense in their medial portion. This intensity tended to decrease from medial to lateral cells, the furthest cells from the central canal, which may be due to the differentiation processes of post-mitotic neurons. We also found this pattern of expression with the col2a1 probe. Conversely, cnfn expression in the grey matter was constant in both the medial and lateral portions of the grey matter. These different expression patterns may be due to the function of each gene during spinal cord development. Interestingly, these genes were also found in spinal cord neurons from

developing mice (Sox2: Petit A, 2011; col2a1 and cnfn: https://mouse.brain-map.org/) which indicate that they are conserved in these two species.

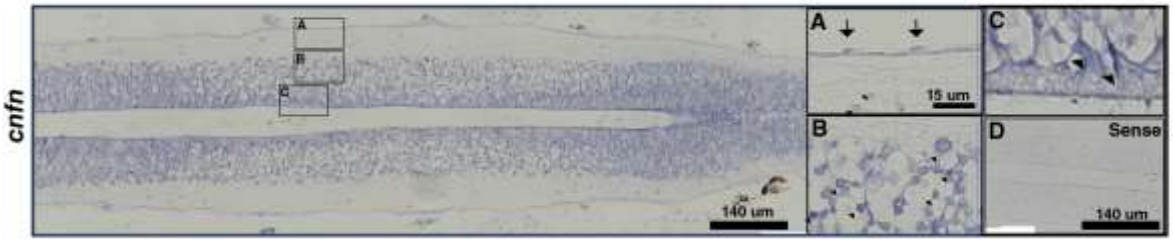


Figure 5. Cnfn RNA expression in the spinal cord of regenerative animals. *In situ hybridization* in longitudinal sections from stage 50 animals. **A-C** show magnifications of the boxed areas: A) meninges, B) grey matter and C) central canal, Big arrows in A) correspond to meningeal cells of the pial layer. Small arrows correspond to cellular bodies found in white matter. Boxed area in C) ependymal prolongation from the central canal.

*4.1.1.3.- Western blot analysis*

To study the expression of cnfn protein, we begin our work using commercial antibodies against the human and the mouse protein. But none of them provided positive and reliable results for *Xenopus* samples. For this reason, we decided to prepare a specific antibody for *Xenopus* cnfn (Figure 6) The peptide chosen is near the amino portion of the protein and has a 91% homology between cnfn 1.a. and cnfn 1.b.

Due the lipophilicity of cnfn we extracted the protein from *Xenopus* tissues by homogenization using SDS-PAGE buffer, as described in Wagner et al., 2019, and we compared to RIPA, triton x-100 (Figure 7), and urea 8M (Figure 8).

To choose the tissues to prepare the samples for these experiments, we analyzed the literature. Cnfn expression has been described in the human epidermis (Michibata et al., 2004), oral mucosa (Wagner et al., 2019), cornea (Choi et al., 2014), and in *Xenopus laevis* spinal cord (Lee-Liu D et al., 2014). From this last work, we also know that the abundance of transcripts is higher in NF- 50 than NF- 66 (Lee-Liu D et al., data not published), which we confirmed here with RT-qPCR assays (Figure 2). Based on this, we decided to test the antibody in the spinal cord, skin, and eye from stage 50 animals and compared SDS-PAGE, RIPA, and triton x-100 as lysis buffer to extract cnfn from these tissues (Figure 6). Consistently, the SDS-PAGE buffer was the best buffer for extracting the protein from the three tissues, followed by RIPA, whose extraction efficiency to cnfn was lower. With Triton x-100, we barely detected any band, and the ones that appeared were heavier than the weight expected for cnfn. In the three tissues studied, we found a

more intense band at 15 kDa approximately, extracted with SDS-PAGE buffer, that might correspond to cnfn, whose theoretical weight is 12 KDa. In order of abundance, we found that the eye and skin had the highest quantity of cnfn compared to the spinal cord.


Figure 6. Homology sequence between cnfn a and b (111 amino acids). Underline letters show the homologs amino acids, which reach 91% of identity. In yellow are shown the 15 cysteine residues that cnfn have. In the blue square is shown the sequence of the antibody made for the study of this protein.

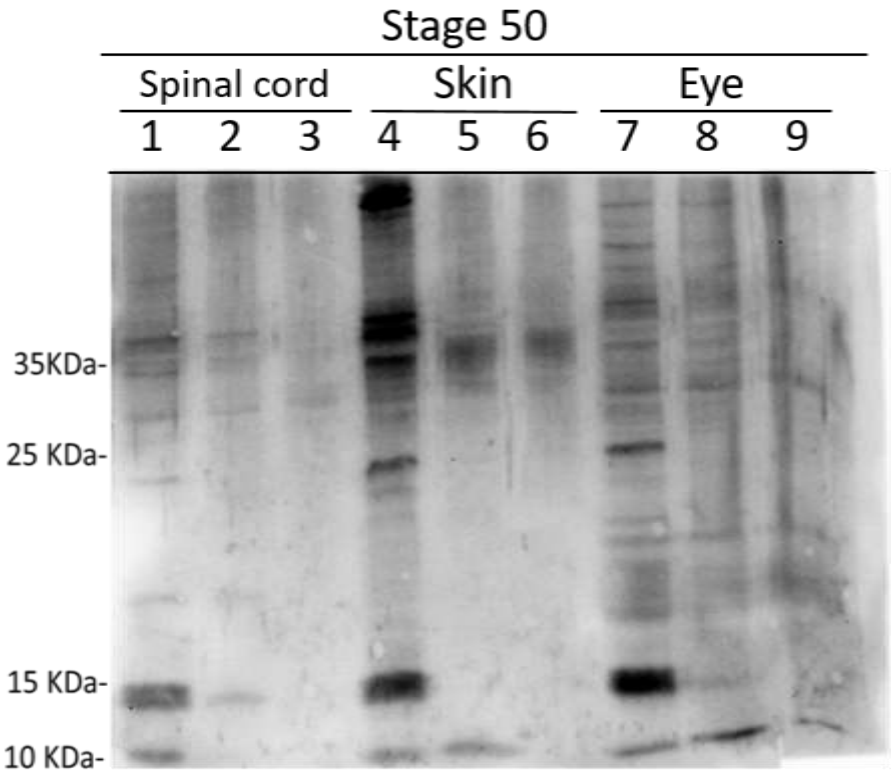


Figure 7. Protein extraction of cnfn in three different tissues of the regenerative stage of *Xenopus laevis*. Extraction of cnfn with SDS-PAGE buffer 1x (lanes 1, 4, and 7), RIPA (lanes 2, 5, and 8), and Triton x-100 (lanes 3, 6, and 9) in the spinal cord, back skin, and eye isolated from stage 50 animals. We refer to cnfn as the 15 KDa band.

We then compared SDS-PAGE lysis buffer to urea 8M to extract cnfn in the spinal cord, eye, and skin (Figure 8). We found that this buffer was also very efficient in extracting the protein from these three tissues, but, again, we found more intense bands with SDS-PAGE. For this reason, we decided to use this buffer in the rest of our work to study cnfn.

In both experiments (Figures 7 and 8), we found that the spinal cord had the lowest abundance of cnfn.

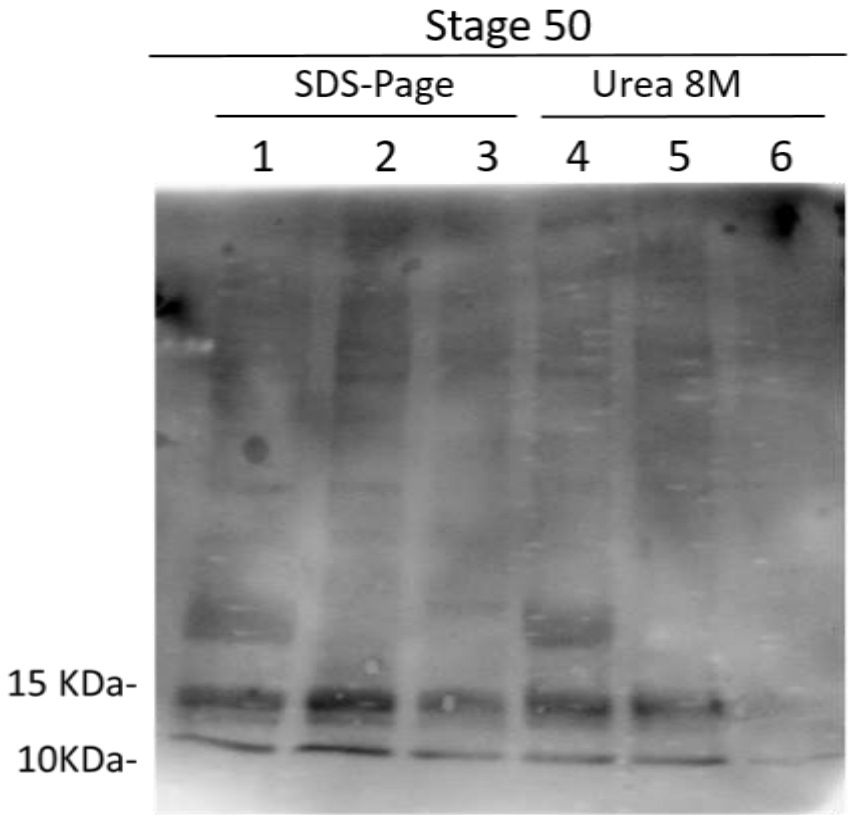


Figure 8. Protein extraction of cnfn comparing two lysis buffers in different tissues of the regenerative stage of *Xenopus laevis*. Comparison of buffer SDS-PAGE 1x and Urea 8M in extracting cnfn from the eye (lanes 1and 4), skin (lanes 2 and 5), and spinal cord (lanes 3 and 6) from stage 50 animals. We refer to cnfn as the 15 KDa band.

To study the protein expression of cnfn in the spinal cord during metamorphosis, we isolated the spinal cord from NF- 50, 54, 58, and 66 animals. We homogenized the samples in 1x SDS-PAGE buffer and assured the good homogenization of the samples with vortex and up-and-down with the pipette before taking the volume used.

We found four bands ranging the weights between 10 and 25 kDa (Figure 9). According to the ncbi for the human gene, cnfn suffers alternative splicing producing two functional protein isoforms, one with 160 amino acids and the other with 112, which gives a weight of approximately 17,6 and 12 KDa (Thierry-Mieg D, 2006). Due to the migration of our protein, we think the 10 KDa band corresponds to the 12 KDa isoform, the band b of 15 KDa corresponds to the 160 amino acid isoform, the band c corresponds to a post-translational modification of cnfn (15-25 KDa), as this protein in mice is palmitoylated in at least five cysteine residues (Liu et al., 2015). Finally, we believe the heaviest expression corresponds to a protein-protein interaction.

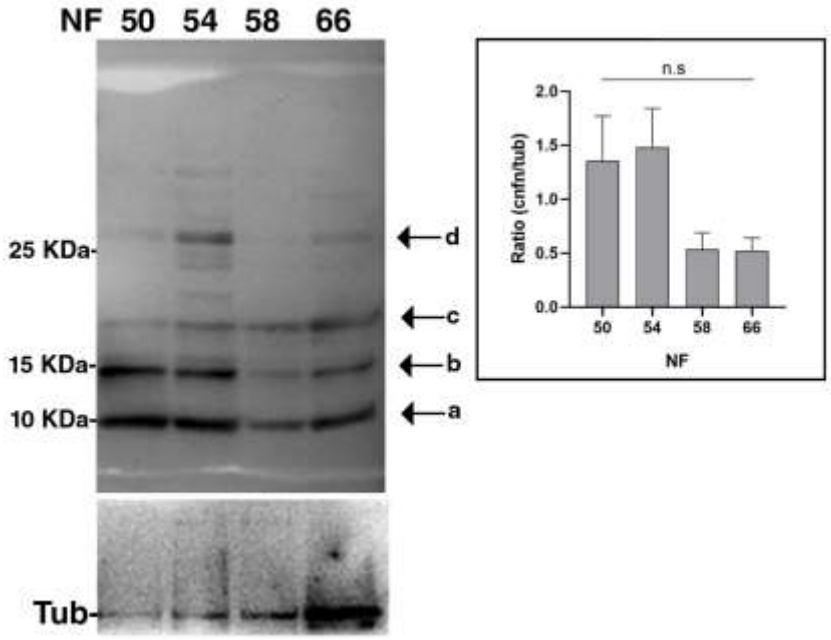


Figure 9. Expression of cnfn in *Xenopus laevis* spinal cord during metamorphosis. Fifteen animals for NF-50 and NF-54 stage, ten for NF-58, and three NF-66 were used to isolate the spinal cord. Tubulin was used as the loading control. Arrow a) show the bands at 10KDa, arrow b) at 15 KDa, c) the one between 15 and 25 KDa and d) at 25 KDa. The inset show the quantification of four different assays against the charge control protein Tubulin. The statistical analysis One-way Anova with multiple comparisons did not found statistical differences between the groups.

Because of the multiple bands that we obtained in our results, we studied the effect of using Urea 2x as a pre-incubation step before loading the samples in the electrophoresis gel. This incubation should reduce the interactions between the proteins and maintain them in their unfolded form. We thought that using this protocol would allow us to identify better the band corresponding to cnfn because multiple bands have not been described in the literature (Michibata et al., 2004; and Wagner et al., 2019). We studied three different stages: 50, 58, and 66. We found four main bands (Figure 10). Bands "a" and "b" migrated between 10 and 15 kDa and tended to decrease their intensity from NF-50 to NF-66. On the contrary, band "c", approximately at 15 kDa, showed an increasing intensity from NF- 50 and NF-58 but a decrease comparing NF- 58 and NF-66. At 25 kDa, band "d", we found a very intense band only for NF- 58. If we compared by stage, we observed that in NF-50, a low-weight cnfn abounds, and in older stages like NF-58, there is a greater abundance of the medium-weight version of this protein.

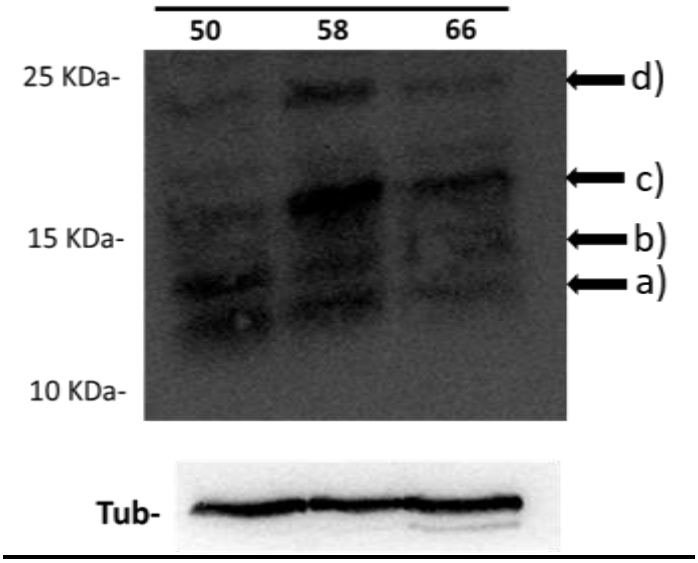


Figure 10. Effect of urea 2x treatment for cnfn expression in different stages of *Xenopus laevis*. Fifteen animals for NF-50, ten for 58 stages, and three for NF-66 stage were used for the protein assays. Tubulin was used as the loading control. Arrow a and b shows the bands that weight between 10 and 15 kDa, arrow c shows the ones that weight 15 KDa and arrow d shows the bands that weight approximately 25 KDa.

*4.1.1.4.-Immunohistochemical analysis*

To further study the protein localization in the spinal cord during metamorphosis, we performed immunohistochemistry assays in stages 50, 58, and 66. In NF-50 (Figure 10), cnfn was widely distributed in the dorsal and ventral grey of the spinal cord. Several degrees of immunoreactivity were observed from a rostrocaudal extent and from medial to lateral regions. Neurons from cervical and thoracic sections were more abundantly labeled than at lumbar levels, where the intensity decreased. At the grey matter, a gradient of expression was observed for cnfn labeled neurons, ranging from weak labeling at medially localized cells to more intense in lateral regions (Figure 11b), suggesting that cnfn is expressed in more differentiated cells. The motor neurons showed the typical phenotype of larger cells bodies with visible nucleolus at the ventral horn. They were also immunoreactive (Figure 11c and g).

Immunoreactivity to cnfn was also found in cells from the central canal. This expression was concentrated in the ventral portion of this structure and presented a gradient ranging from cervical (most intense) to lumbar sections (weakest labeling) (Figure 11d, i and, l).

Cells from the pial layer were also immunoreactive to cnfn (Figure 11h) and were found surrounding the neural tissue in all the rostrocaudal axis.

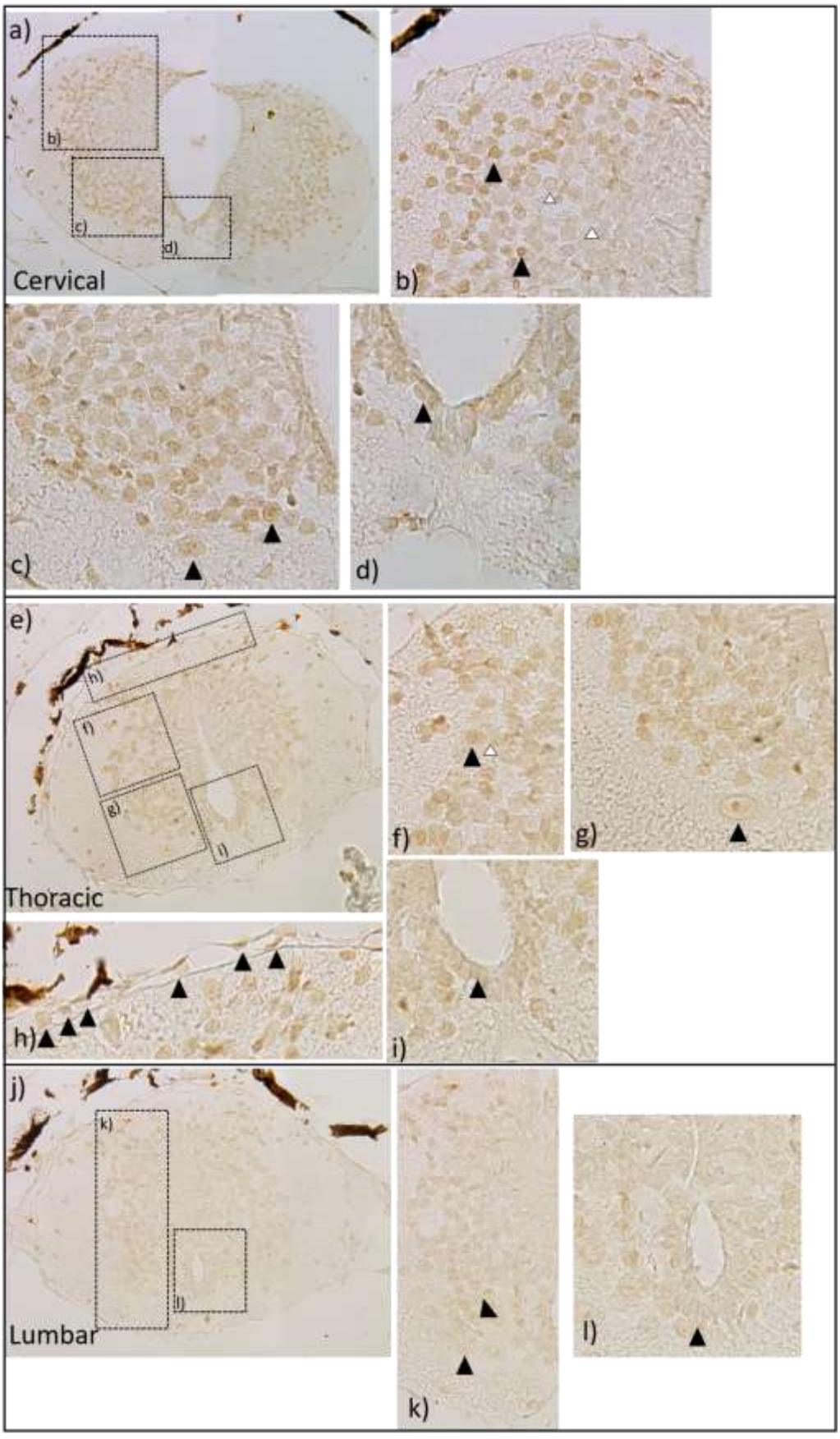
a)
b)
c)
d)
Cervical
b)
c)
d)
e)
h)
f)
g)
i)
Thoracic
f)
g)
h)
i)
j)
k)
l)
Lumbar
k)
l)

Figure 11. Cnfn expression in the spinal cord of regenerative animals. Immunohistochemistry in transversal sections from NF-50 animals. **a)** cervical section. b-d show magnifications of the boxed areas. In b) dorsal region, black arrow-heads point to dorsal neurons with punctate or full expression for cnfn. White arrow-heads show neurons with less or no expression. c) ventral region, black arrow-heads point to ventral neurons that showed nucleolus. d) ependymal cells in the ventral region of the central canal. Black arrow-head points to a cnfn positive cell. **e)** Thoracic section. f-i show magnifications of the boxed areas. In f) dorsal region, black arrow-head show a dorsal neuron with full expression of cnfn. White arrow-head show a dorsal neuron with less or none labeling for cnfn. g) ventral region, black arrow-head point to a ventral neuron nucleolus. h) pial cells from the meninges sorrounding the neural tissue. i) ependymal cells of the ventral region of the central canal. Black arrow-head shows a cnfn positive cell. **j)** Lumbar section. K) and l) shows magnifications of the boxed areas. k) dorsal and ventral region, black arrow-heads show neurons with punctate expression in the ventral region. l) ependymal cells in the ventral region of the central canal. Arrow-head points to an ependymal cell with less expression of cnfn.

In NF-58 (Figure 12), the expression intensity of cnfn was reduced compared to NF-50. Positive cells from the grey matter were found widely distributed. Unlike NF-50, the intensity of the signal in the grey matter was homogenous in dorso-ventral and in medial to lateral regions.

The pial cells showed more robust labeling for cnfn than in NF-50 (Figure 12b-c). These cells had a more elongated shape than neurons and were in close apposition to the spinal cord tissue. Arachnoid cells were also immunoreactive to cnfn (Figure 11b-c, arrowheads).

In the central canal (Figure 12e), immunoreactivity was found in ependymal cells from the mid and ventral regions. The labeling was very weak, but we were able to observe some ependymal cells positive to cnfn.

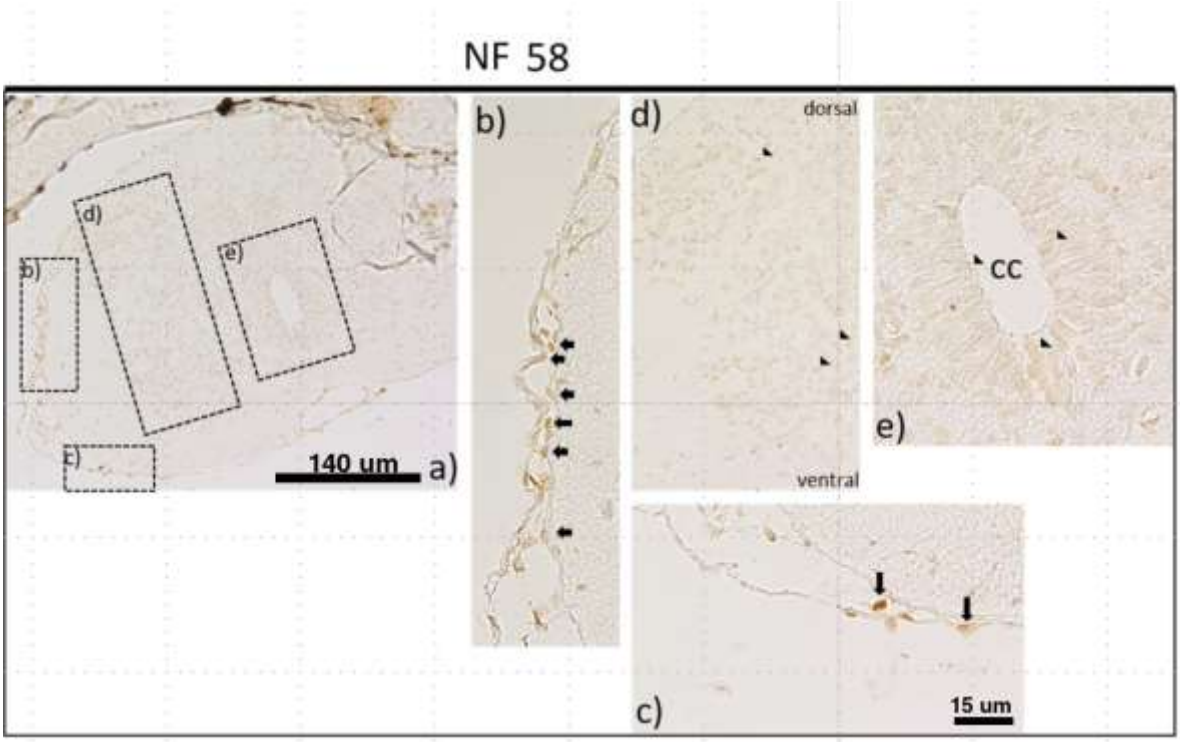


Figure 12. Cnfn expression in the spinal cord of non-regenerative animals. Immunohistochemistry in transversal sections from NF-58 animals. **a)** thoracic section. b-e show magnifications of the boxed areas. In b-c) pial cells surrounding the neural tissue of the spinal cord. Single cells are detectable and immunoreactive to cnfn. d) dorsoventral magnification. Arrow-heads show positive neurons from the grey matter. e) Arrow-head shows immunoreactivity on ependymal cells from mid-and ventral regions of the central canal.

In NF-66 (Figure 13), a rostrocaudal gradient was found in serial sections from thoracic to lumbar levels. In thoracic sections (Figure 13a and d), a weaker immunoreactivity was detected. We observed scarce neurons positive to cnfn in the dorsal grey matter. In the ventral region, motor neurons were labeled too. They were larger and clustered at the ventral horn. Descending in the rostrocaudal axis, the labeling became more intense (Figure 13g). The immunoreactivity to cnfn was homogenous both from dorsal to ventral and medial to lateral regions.

As in previous stages, we found pial cells positive to cnfn (Figure 13h).

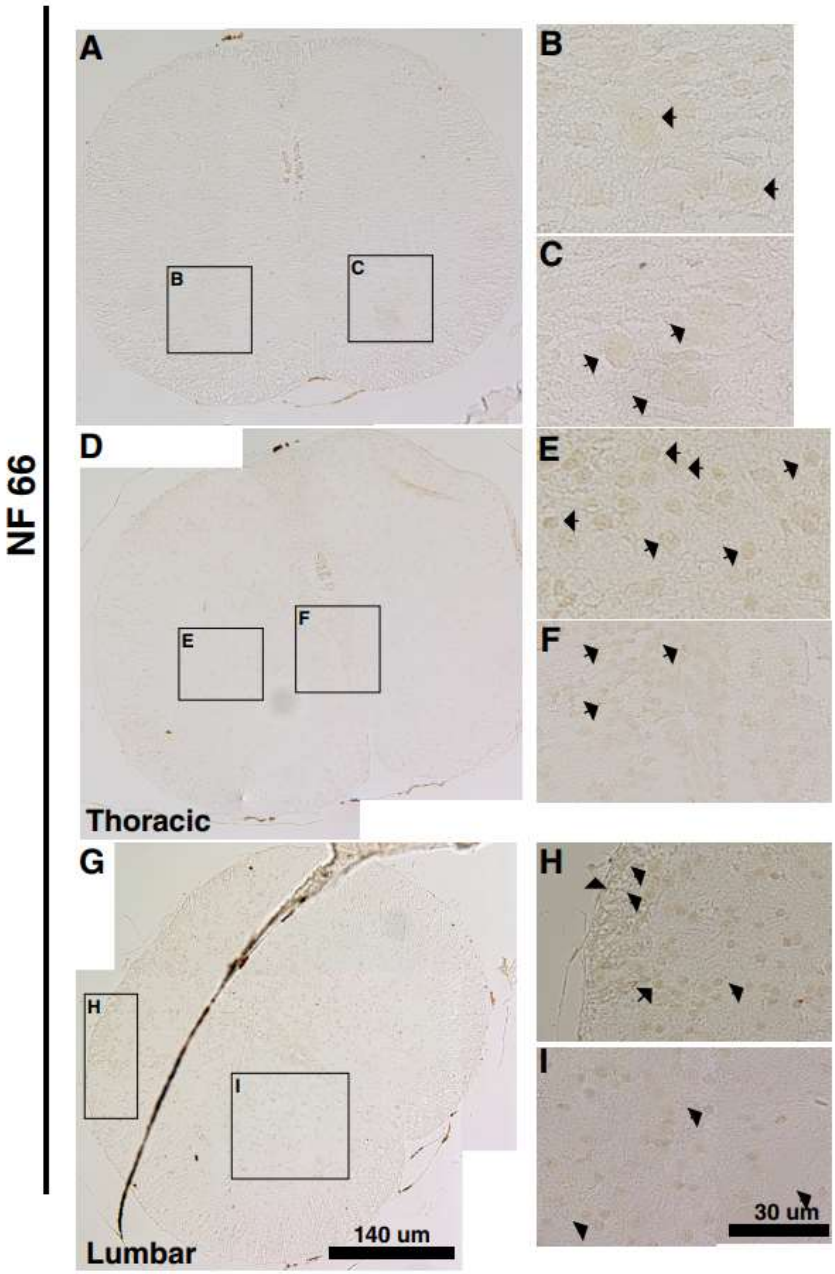


Figure 13. Cnfn expression in the spinal cord of non-regenerative animals. Immunohistochemistry in transversal sections from NF-66 animals. a)-d)-g) thoracic to lumbar sections. b-c) shows the magnification of the boxed areas in a). b) and c) Immunoreactive neurons from the ventral grey. e-f) shows the magnification of the boxed areas in d). Arrows show the wide distribution of neurons from the medial portion of the grey matter immunoreactive to cnfn. h-i) shows the magnification of boxed areas in g). h-i) Arrow-heads show the wide distribution of immunoreactive neurons from the dorsal and ventral grey.

### *4.1.2.- Eye expression*

#### *4.1.2.1.- RT-qPCR analysis*

As cnfn expression in the eye was strongly detected by western blot in NF-50 and the literature locate cnfn on the cornea (Choi et al., 2014), we decided to explore this expression throughout metamorphosis. We tested mRNA levels in NF-50, 54, 58 and 66. The mRNA levels of cnfn were normalized to the housekeeping gene *eef1a1*.

The levels of cnfn were low from NF-50 to NF-54 and increased significantly after metamorphosis at NF-66 (Figure 14). Interestingly, contrary to what we observed in the spinal cord, the biological variability of cnfn in the eye was notably lower with the exception of NF-58.

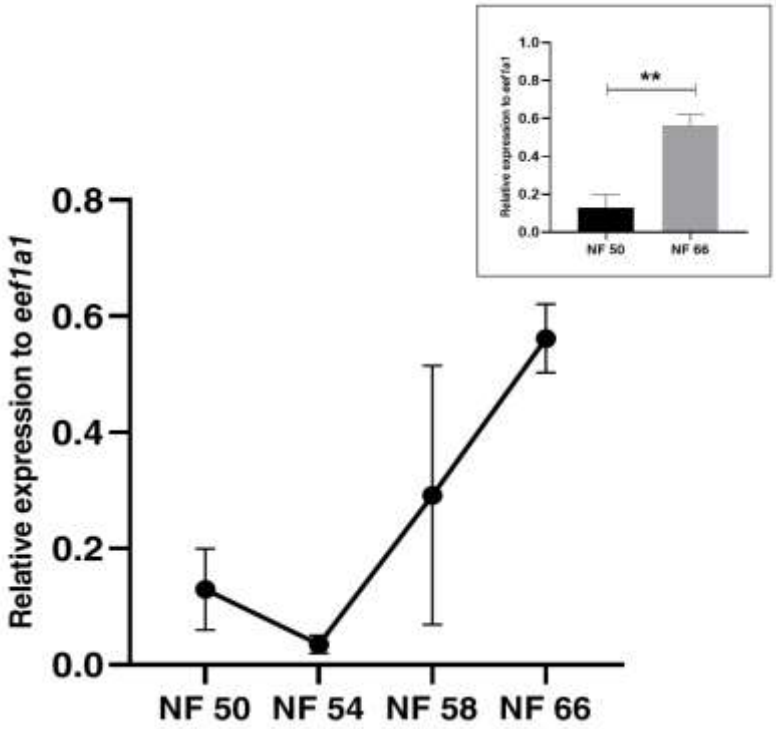


Figure 14**.** *Cnfn* RNA levels in the eye during *Xenopus laevis* metamorphosis. *Cnfn m*RNA levels detected by RT-qPCR were normalized against *eef1a1* (average ± SEM, n=3 for all the stages studied). The inset show the comparison of the levels of cnfn between stages 50 and 66. A double-tail t-test between these stages found a statistical difference (p=0.0092).

*4.1.2.2.- in situ hybridization*

Using *in situ hybridization* in paraffin-embedded eyes from NF-50 animals, we found that cnfn antisense probe hybridized in the ganglion cell layer and in the outer nuclear layer of the retina (Figure 15), where the cell body of the photoreceptors lies. In the ganglion cell layer, which is a very heterogeneous layer, the expression of cnfn was even and strong.

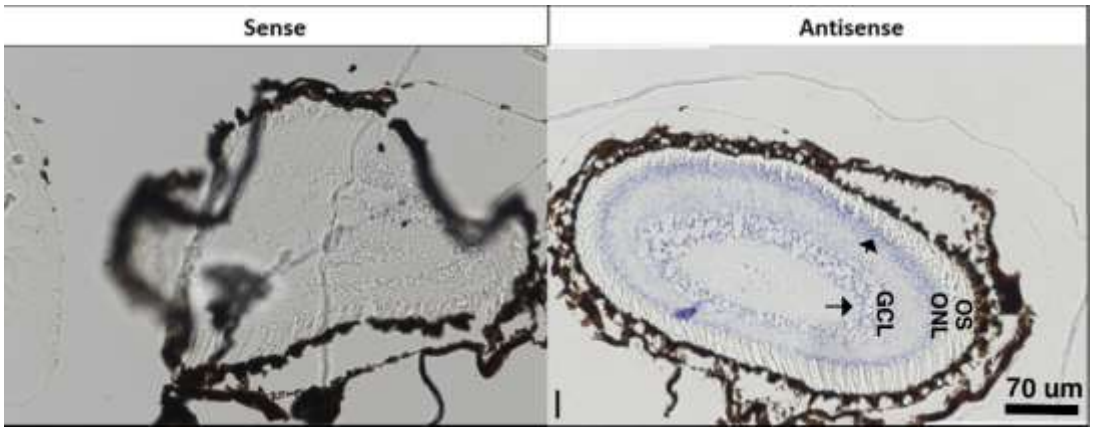


Figure 15. Cnfn RNA expression in the eye of regenerative animals. *in situ hybridization* in longitudinal sections from NF-50 animals for sense and antisense probes. GCL: ganglion cell layer. ONL: Outer nuclear layer. OS: Outer segment.

*4.1.2.3.-Western blot analysis*

We studied the protein expression of cnfn in the eye during metamorphosis as well. We isolated the eyes from NF-50, 54, 58 and 66 and homogenizated them in SDS 1X. Contrary to what we observed in cnfn mRNA levels, we found a tendency to decrease its levels from NF-50 to NF-66 (Figure 16). This discrepancy may come from a higher regulation of cnfn translation or a higher protein turnover in froglets, so new mRNA is constantly synthesizing.

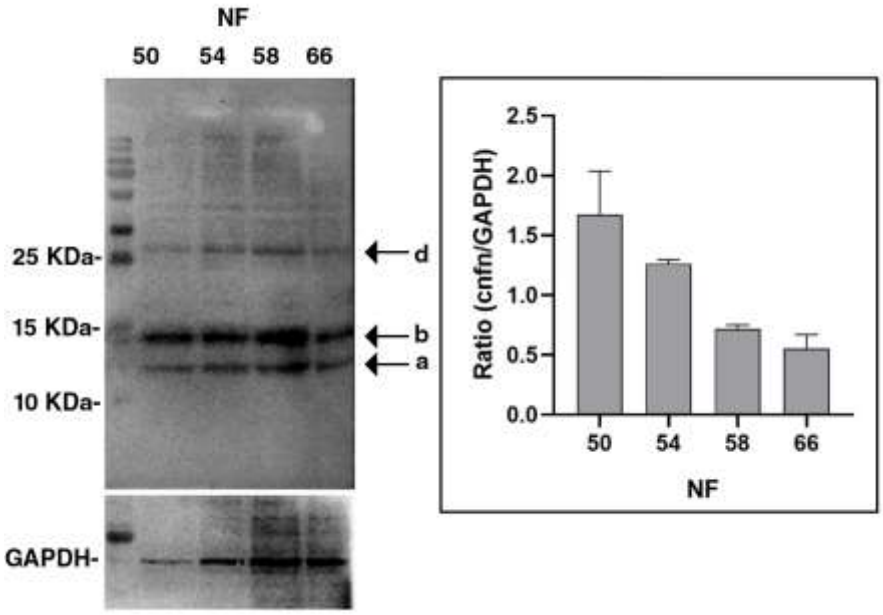


Figure 16. Expression of cnfn in *Xenopus laevis* eye during metamorphosis. Four animals for NF-50 and NF-54 stage, 3 for NF-58 and 66 were used to isolate the eye. GAPDH was used as the loading control. Arrow a) show the bands above 10KDa, arrow b) the band at 15 KDa, and arrow d) the bands that weight 25 kDa. The inset show the quantification of two different assays against the charge control protein GAPDH.

*4.1.2.4.- Immunodetection analysis*

The expression of cnfn was also evaluated with immunofluorescence and immunohistochemistry assays. In contrast to what we obtained with spinal cord sections treated for immunofluorescence, in eye cryosections, cnfn was detected and found in the photoreceptor layer of the retina from NF-50 to NF-66 (Figure 17). The photoreceptor layer consists of several folding membranes that form the cellular body. We detected a decreased in the immunoreactivity from NF-50 to 66. In addition, cnfn expression changes its localization from NF-50 detected on the cell bodies of the photoreceptor layer to a membrane expression on NF-54 and NF-58.

In immunohistochemistry assays we studied the expression in NF-50 and NF-66 (Figure 18). Cnfn immunoreactivity was found on several layers of the retina as the outer segment (OS), outer nuclear layer (ONL), inner nuclear layer (INL), and ganglion cell layer (GCL) in both stages with a decrease in the intensity on GCL layer on NF-66.

We also found immunoreactivity in the inner and outer layer of the cornea and in the stroma (Figure 19).

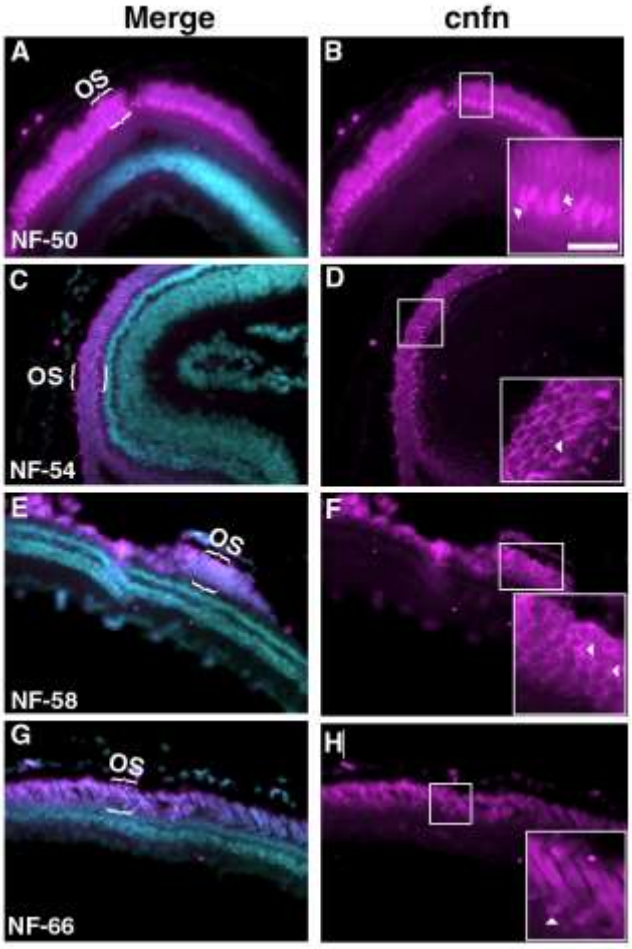


Figure 17. Cnfn expression in the retina during the metamorphosis of *Xenopus laevis*. Immunofluorescence in paraffin sections of *Xenopus* retina at four different stages during metamorphosis (A-H). Nucleus were stained with Hoechst. OS: Outer segment. The colors were manually changed to cyan and magenta according to color friendly guides.

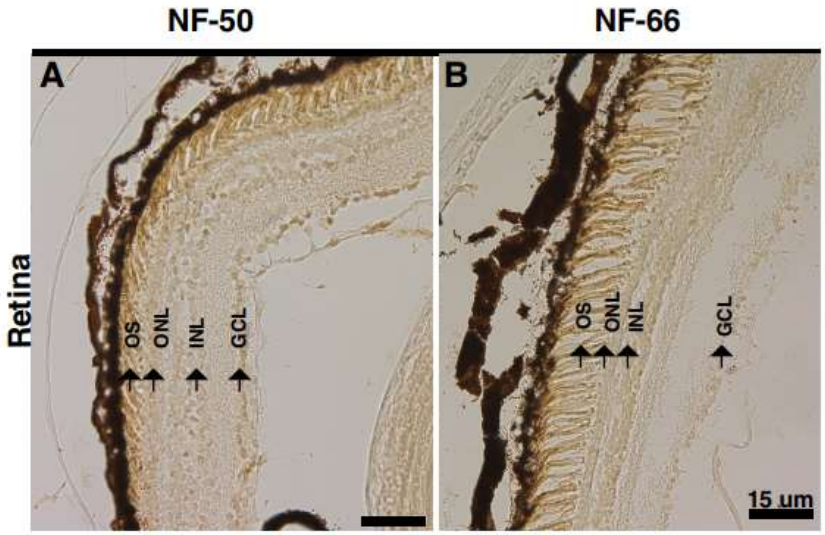


Figure 18. Cnfn expression in the retina of regenerative animals. Immunohistochemistry in transversal sections from NF-50 and NF-66 animals. Cnfn (1:100 dilution) was developed with DAB peroxidase HRP kit for five minutes. GCL: Ganglion cell layer. INL: Inner nuclear layer. ONL: Outer nuclear layer. IS: Inner segment. OS: Outer segment.

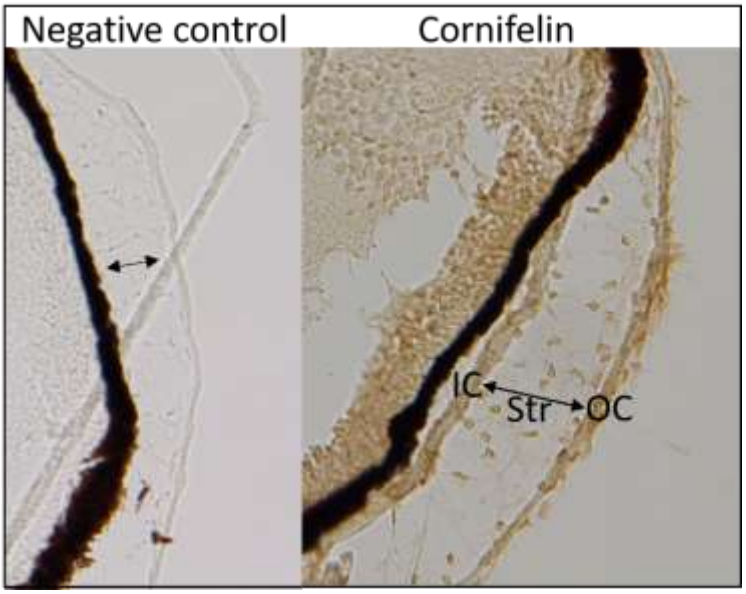


Figure 19. Cnfn expression in the cornea of regenerative animals. Immunohistochemistry in transversal sections from NF-50 animals. Negative control was processed with the treated sections but was not incubated with the primary antibody. Cnfn (1:100 dilution) was developed with DAB peroxidase HRP kit. The two-headed arrow shows the extension of the stroma (Str). IC: Inner cornea. OC: Outer cornea.

### *4.1.3.- Cnfn expression after spinal cord injury in R and NR-stages*

#### *4.1.3.1.- RT—qPCR analysis*

In a previous study of our lab (Lee-Liu D, 2014), the injury response for both R- and NR-animals after transection was evaluated by high throughput mRNA sequencing. The results showed that cnfn is one of the most differentially expressed transcripts in NR-stage two days the after injury and down-regulated that same day in R-stage animals (Lee-Liu et al. 2014).

To further investigate the response of cnfn to injury, we performed RT-qPCR at 21 hours, and 2, 6 and 10 days after injury by transection. We compared the results to sham-operated levels in R and NR-animals (Figure 20). In R-animals (Figure 20a), the levels of cnfn did not changed after the injury. In NR-animals (Figure 20b), the levels of cnfn were already upregulated more than two times at 21 hours after transection. They remained upregulated until day six after injury, attaining almost four times of increase compared to sham animals. Ten days after injury, the levels returned to those observed in control animals.

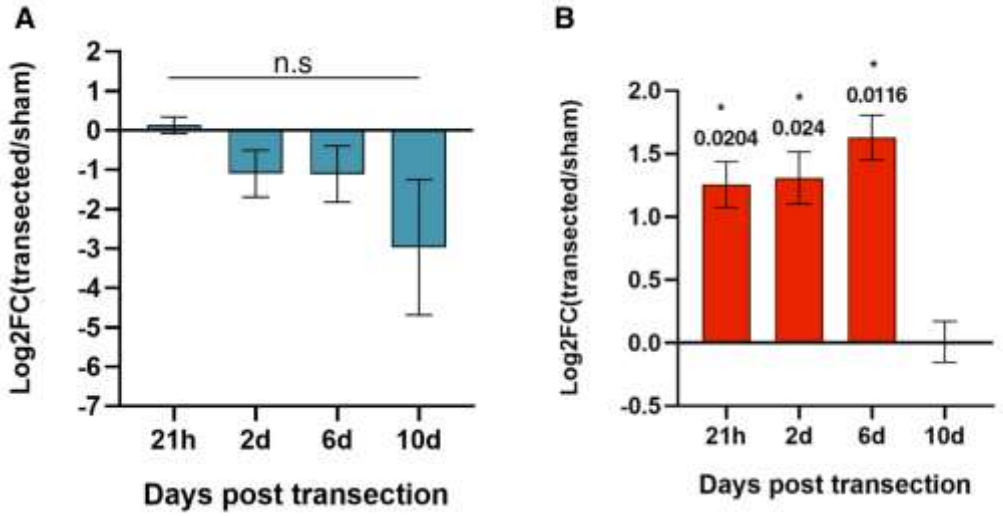


Figure 20. *Cnfn mRNA* levels after spinal cord injury by transection in A) NF-50 and B) NF-66 (four independent assays for each stage). Bars represent the average ± SEM. Cnfn mRNA levels were normalized against *eef1a*, and the ratio between transected and sham-operated animals. The log2 of each ratio was calculated and graphed. The one sample t and Wilcoxon test was performed for each stage, against an hypothetical value =0. For NF 50, the analysis did not found any statistical difference. For NF-66 the differences are shown for each condition, *$p<0.05$.

*4.1.3.2 Western blot analysis*

We took the same temporal window to study the protein levels after injury and compare them with sham levels at day one (Figure 21). The blot presented represent four independent assays and the inset shows the quantification of the intensity levels of cnfn normalized to tubulin. We found two expression bands for R-stage, one between 10 and 15 kDa and the other at 15 KDa. As the mRNA levels, the protein did not change significantly after the injury.

For NR-stage (Figure 22), the result represents four independent assays. The inset shows the quantification of the intensity of cnfn normalized with tubulin. We got four expression bands, two stronger than the others (between 10 and 15 KDa and the other at 15 KDa), and two less intense (at 10 KDa, and at 25 KDa). The statistical analysis did not found differences between the conditions.

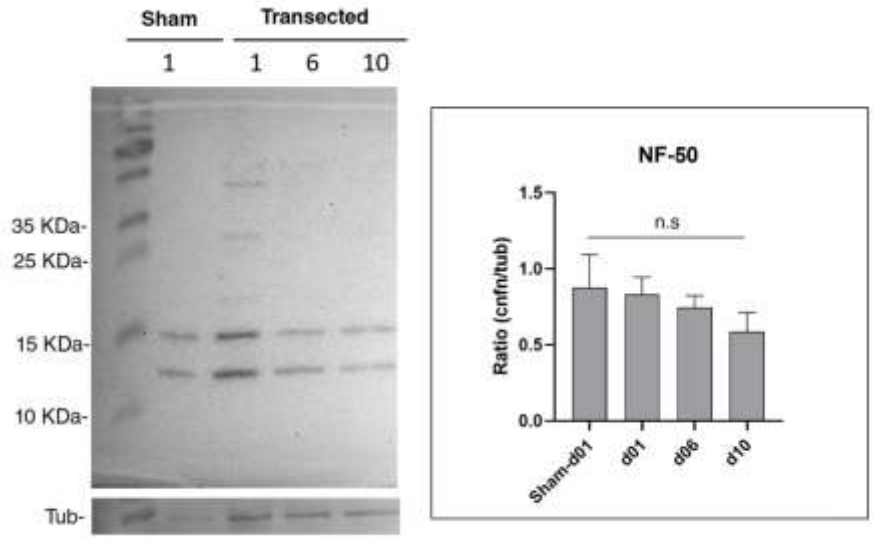


Figure 21. Expression of cnfn after spinal cord injury in R-animals. Spinal cords of NF-50 animals were isolated at 1-day post sham surgery, and at 1, 6 and 10 days after transection injury. Fifteen animals were used for each temporal point. Tubulin was used as loading control. The inset show the quantification of four independent assays. The One-way Anova did not found any statistical differences between the groups.

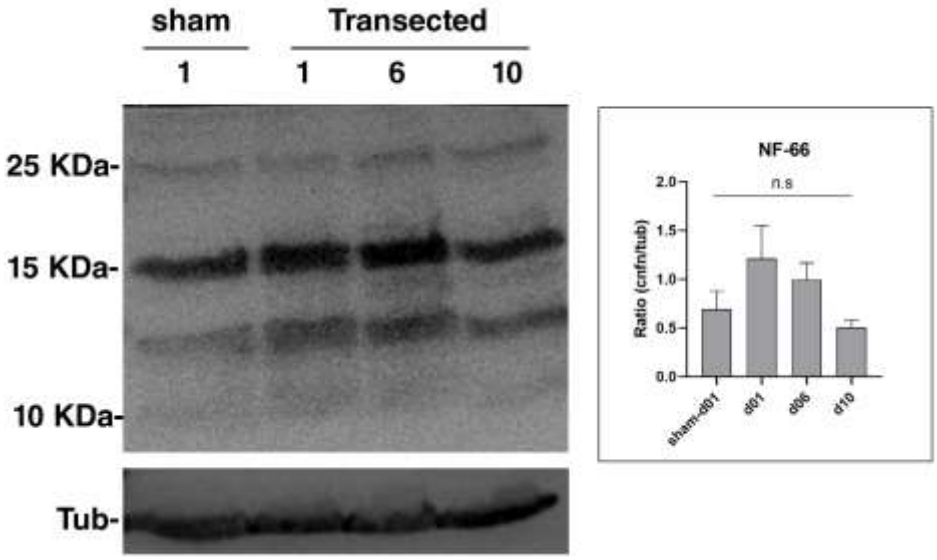


Figure 22. Expression of cnfn after spinal cord injury in NR-animals. Spinal cords of NF-66 animals were isolated at 1-day post sham surgery, and at 1, 6 and 10 days after transection injury. Three animals were used for each temporal point. Tubulin was used as loading control. The inset show the quantification of four independent assays. One-way Anova did not found any statistical differences between the groups.

*4.1.3.3 Immunodetection analysis*

For transverse sections, we analyzed three temporal points (2, 6 and 10 days) after spinal cord injury and compared the cnfn expression with uncut conditions (Figure 23). As we saw before at uncut conditions, cnfn was detected on cells from the gray matter and also found in the pial layer of meninges surrounding the neural tissue (Figure 23a). After the injury, the intensity of cnfn on neurons decreases at the three temporal points analyzed (Figure 22 b, c, and d). The reduction on the intensity is more severe at day 10, where cnfn was found only on meninges (Figure 23 d). The decrease in protein levels is coherent with the mRNA showing that cnfn decreases after the injury and does not return to basal levels at day 10.

On the other hand, the meninges also react to the injury. Pial cells increase their thickness and also the immunoreactivity to cnfn. We were also able to detect it on the dural layer (Figure 23-d1, arrow) which is in close relation with the vertebral process.

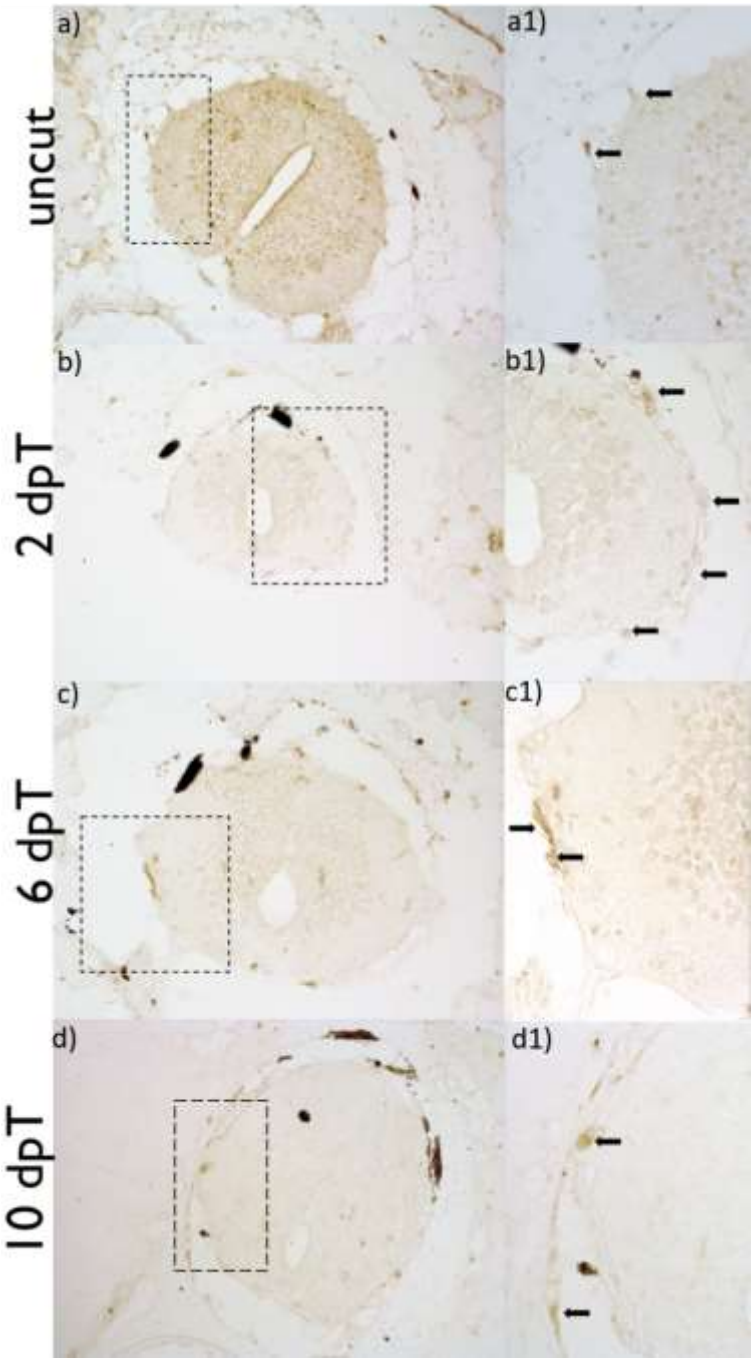


Figure 23. Cnfn expression in R-animals after spinal cord injury. Cnfn immunohistochemistry on transversal sections after 2, 6, and 10 days post transection injury (a-d). Cnfn (1:100 dilution) was developed with DAB peroxidase HRP kit for five minutes. The squared boxes show the area magnified of each corresponding image. The black arrow indicates the expression of cnfn in the meninges.

On longitudinal sections, the meningeal reaction becomes more evident. We studied the cnfn expression on day one, six and ten after the injury. We found an interesting group of cells positive to cnfn one day after the injury (Figure 24a). These cells seemed to be part of the meningeal layer as they have a spindle shape and were found also lining the neural tissue near the injury (Figure 24 b and c). We also detected expression on the grey matter, but the immunoreactivity was less intense. Six days after the injury, the neural tissue is reconnecting, but the central canal had not (Figure 24d). The cnfn positive cells were delineating the neural tissue in reconnection (Figure 24e), and was also possible to observe a group of grey matter cells in reconnection delineated by cnfn positive cells (Figure 24f). Ten days after the injury, the reconnection of the neural tissue seems completed (Figure 24g). The cells positive to cnfn were found on the pial layer and surrounding a group of cells still in reconnection (Figure 24 h and i).

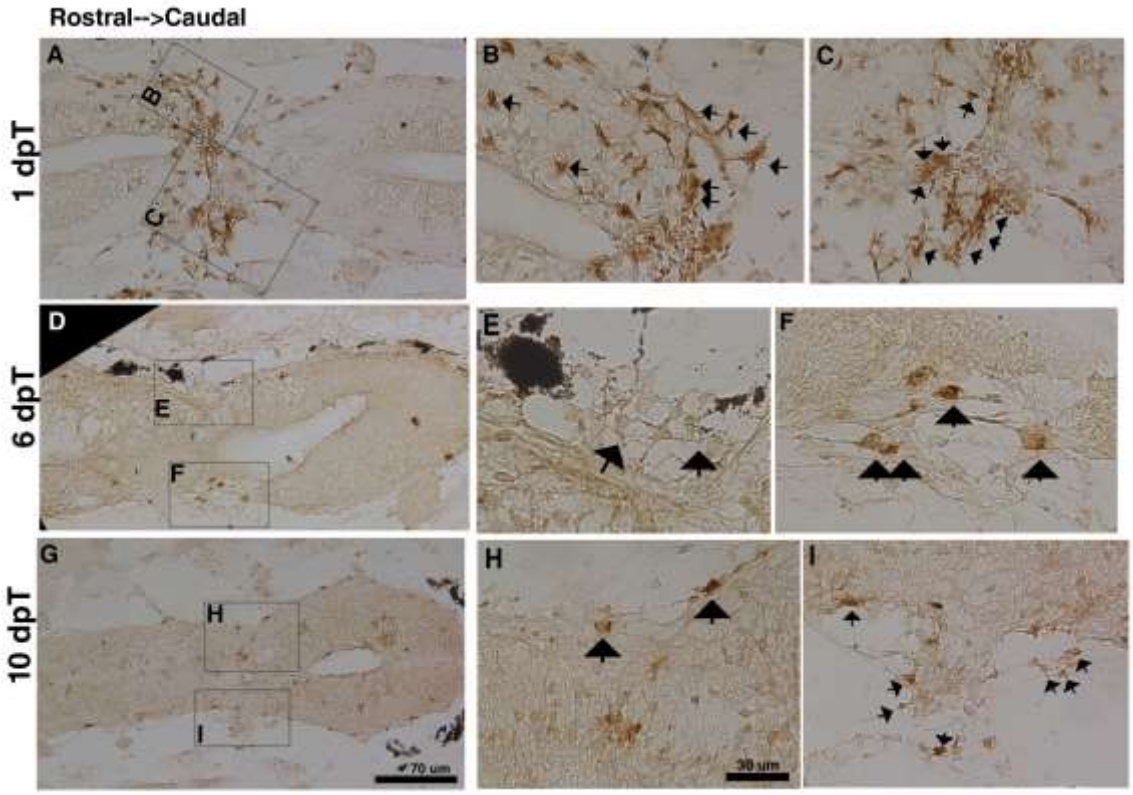


Figure 24. Cnfn expression in R-animals after spinal cord injury. Cnfn immunohistochemistry on longitudinal sections after 1, 6, and 10 days post transection injury (a-i). Cnfn (1:100 dilution) was developed with DAB peroxidase HRP kit for five minutes. The squared boxes show the area magnified of each corresponding image. The black arrow indicates the expression of cnfn in the meninges.

We analyzed the cnfn response after spinal cord injury in NR-animals as well. In uninjured conditions, the immunoreactivity of cnfn on the neural tissue was almost undetectable (Figure 25a). Cnfn expression significantly increased two days after the injury on the grey matter, central canal, and meninges (Figure 25 c and d). The pial cells have thickened, and cnfn labeling is highly enriched in this tissue. On day six after injury (Figure 25e), neural cells positive to cnfn were detected on the dorsal grey area. At ventral regions, cnfn was detected on sparse neurons on the damaged tissue and found on the cellular depositions surrounding the tissue (Figure 25f). Due to the location of this response, the deposition may come from meningeal cells. On day ten (Figure 25g and h), the immunoreactivity has decreased, and the expression can be found on the dorsal and ventral regions of the grey matter. On longitudinal sections on this temporal point, we found the neural tissue separated by a barrier of cells and deposition on the injury site (Figure 25i). Cnfn positive cells were found on the pial layer of meninges surrounding the spinal cord (Figure 25j), and on the injury site, being part of the deposition (Figure 25k).

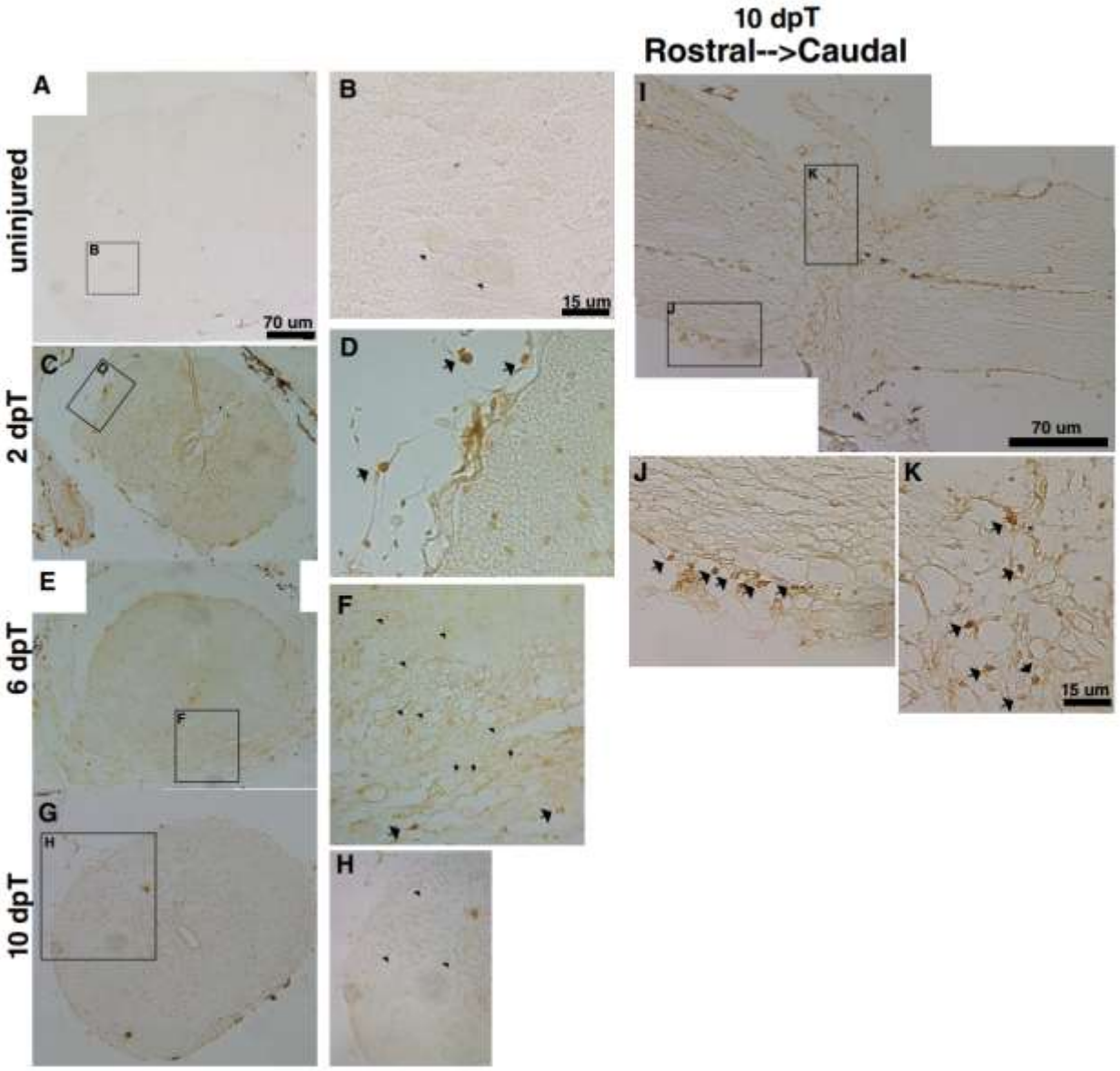


Figure 25. Cnfn expression in NR-animals after spinal cord injury. Cnfn immunohistochemistry on transversal and longitudinal sections after 2, 6, and 10 days post transection injury (a-k). Cnfn (1:100 dilution) was developed with DAB peroxidase HRP kit for five minutes. The squared boxes show the area magnified of each corresponding image. The black arrow indicates the expression of cnfn in the meninges.

#### *4.1.4.1 Meninges reaction after transection injury in R and NR-animals*

As an indirect method to describe the meninges behavior after the injury, we used Masson stain to detect collagen and Hematoxylin & Eosin to describe the reaction of the meninges after the injury. We took NR-animals 2,6 and 10 days after the injury and compared them with control tissue. R-animals in uninjured conditions, did not showed collagen I on the leptomeninges (Figure 26 a-b). Two days after the injury, a thickening on the lateral meninges was observed which did not have collagen fibers (Figure 26 c-d). The thickening of the layers was also observed on the ventral portion of the cord with cells with a spindle shape 6 days after the injury (Figure 26 e-f). The thickening of the layers was reduced 10 days after the injury (Figure 26 g-h). On these latter studied days, we did not detect collagen fibers.

On NR- animals, in uninjured animals, collagen fibers were not detected and the pia was stain on light pink (Figure 27 a-c). Two days after the injury by transection, on Masson results we found the gap full of blood cells (Figure 27 d) and the pia surrounding the neural tissue was also full of them (Figure 27 f). On hematoxylin & eosin results we found some covering on the rostral stump that seems to come from the dura as leptomeninges are lining the neural tissue. There was an increase on extracellular matrix deposition that was also associated with these layers. Ten days after the injury, we still found blood cells on the pial layer (Figure 27 i) and some collagen fibers were near the injury site on the caudal cord (Figure 27 j). The gap between the neural stumps was full with cellular infiltration. There were some cells with spindle shape (Figure 27 k, yellow arrow)

alongside dark nucleus rounded cells, and blood cells. Twenty days after the injury, the infiltration on the gap has cleared and a group of cells were more concentrated on the borders of both stumps (Figure 27 l). Collagen fibers were found on the meninges lining the neural tissue and also on the injury site, associated with the infiltration remaining. On the gap, collagen fibers were also associated with a rosette-like group of cells (Figure 27 n).

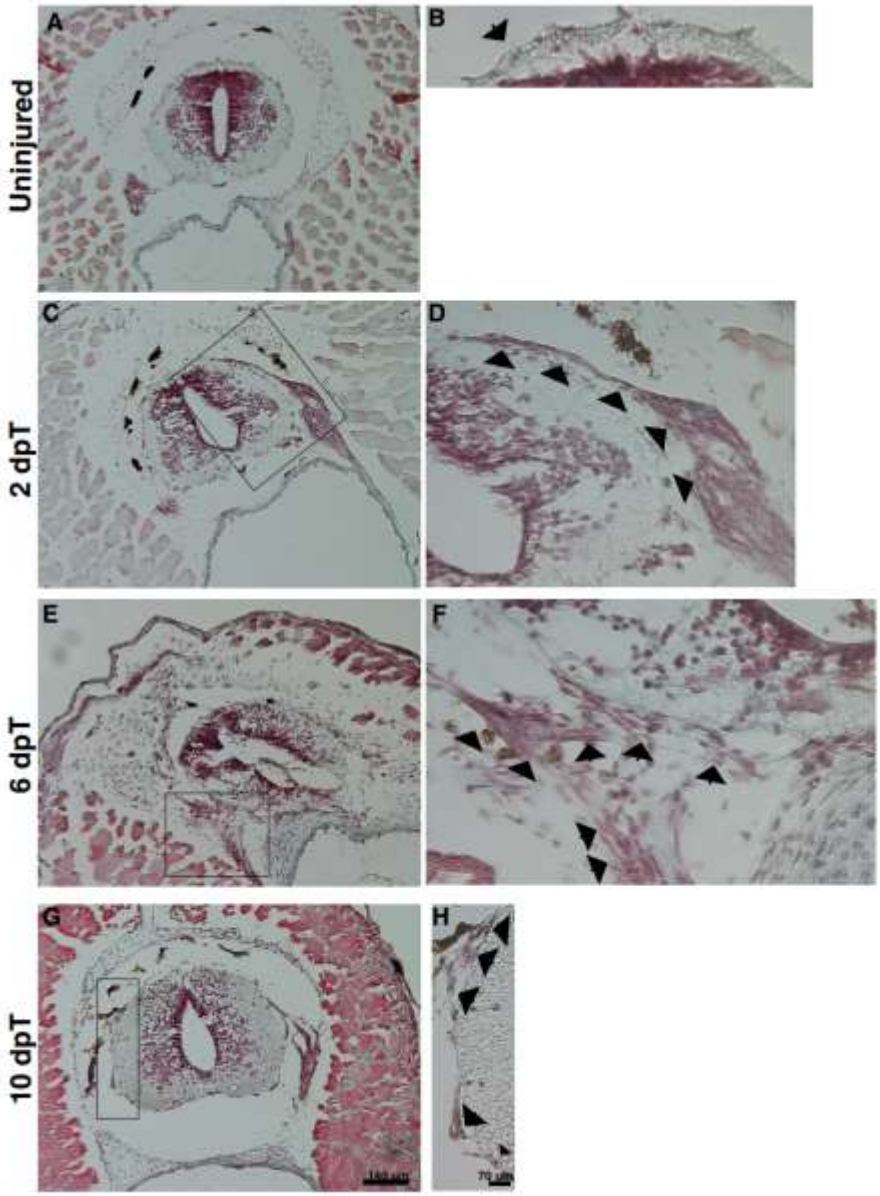


Figure 26. Meningeal reaction after spinal cord injury in R-animals. Spinal cords from NF-50 animals A-B) uninjured, C-D) 2, E-F) 6, G-H) 10 days after injury were stained with masson to evaluated the reaction of the meninges. Boxed areas shows the magnification.

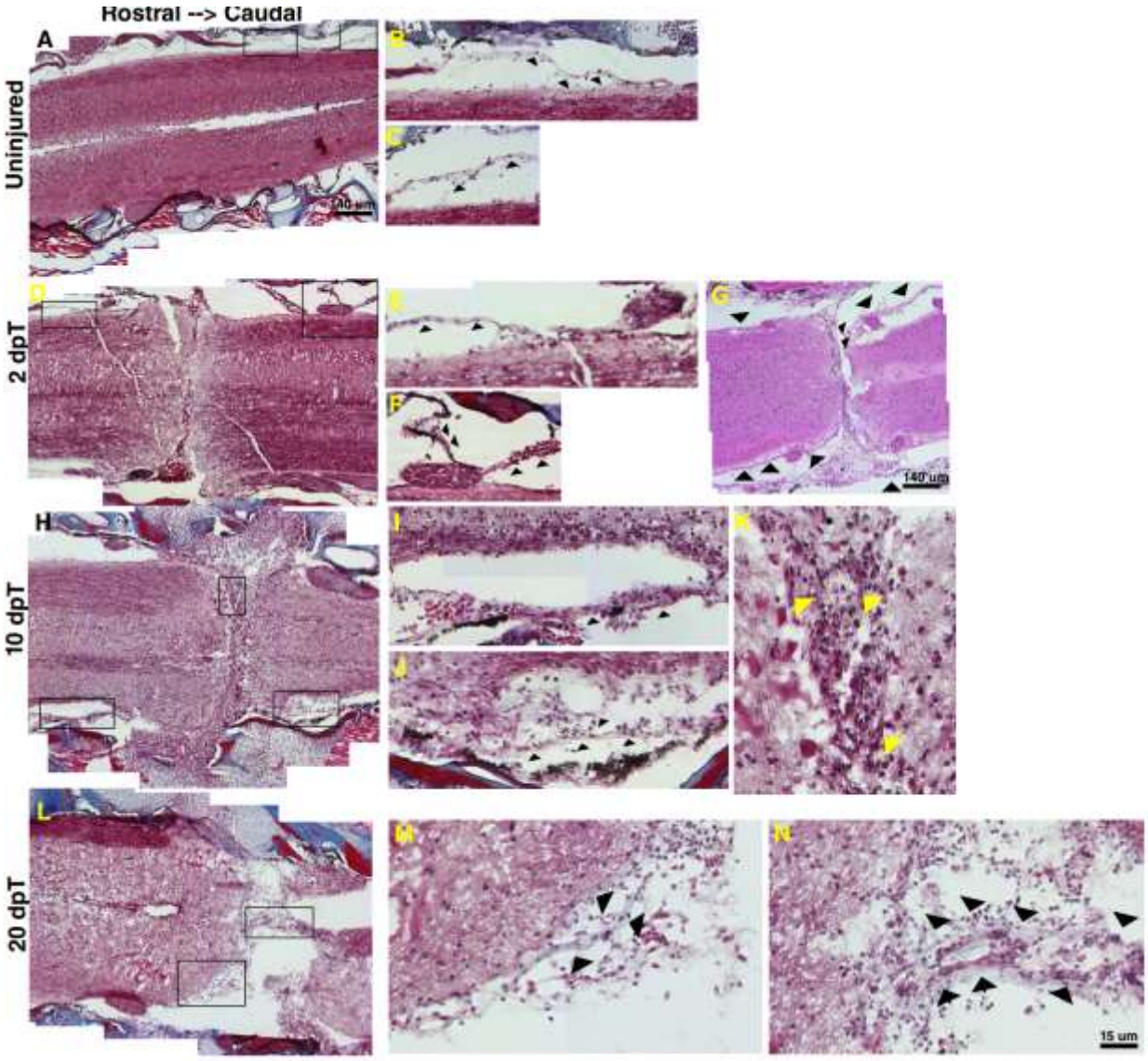


Figure 27. Meningeal reaction after spinal cord injury in NR-animals. Spinal cords from NF-66 A-C) uninjured animals and after D-G) 2, H-K)10 and L-N) 20 days of transection injury were stained with Masson and hematoxylin & eosin staining to evaluated the reaction of the meninges. Boxed areas shows the magnification.

### *4.1.5. Characterization of a transgenic line to cornifelin*

We characterized a transgenic line for cnfn that was prepared in our laboratory (PhD Thesis, Dasfne Lee-Liu). This transgenic line contains the gene cnfn-2A-GFP under the control of the promotor of the heat shock protein 70 (Figure 28a). This line also carries the fusion protein tdTomato under the promotor gamma-crystalline, which allows the selection of the transgenic animals (Figure 28b).

#### *4.1.5.1 Cnfn mRNA induction in the transgenic line after a heat shock*

To check the overexpression of cnfn in this line, we performed RT-qPCR assays with spinal cord samples from F1 offspring tadpoles (NF-50) after one heat shock to induce the transgene expression. The samples were collected at 10 and 24 hours post heat shock (Figure 29). We observed that after 10 hours of the induction, the levels of *cnfn* were 5 times higher than transgenic animals who do not receive the heat induction. Moreover, when the samples were collected at 24 hours post the induction, the levels were 2 times higher than the animals without the induction. These decreased levels suggest a temporal frame for the induction.

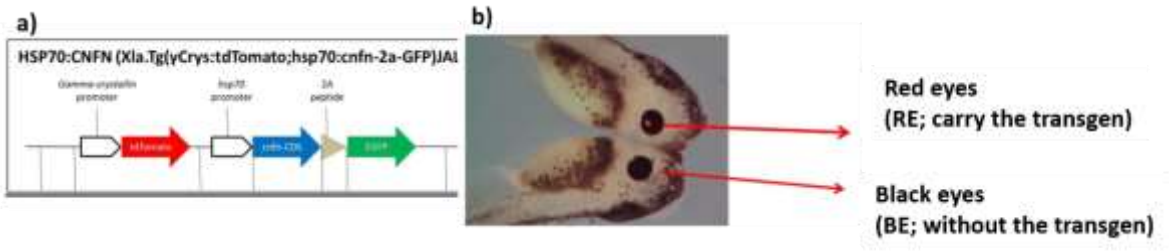


Figure 28. Cnfn transgenic line. A) construct of the transgene is formed by the gamma-crystallin promoter that induce the expression of the red protein tomato in the crystallin of the animals, B) which is used for the selection of the animal groups. The overexpression of *cnfn* is induced by the heat shock 70 promotor.

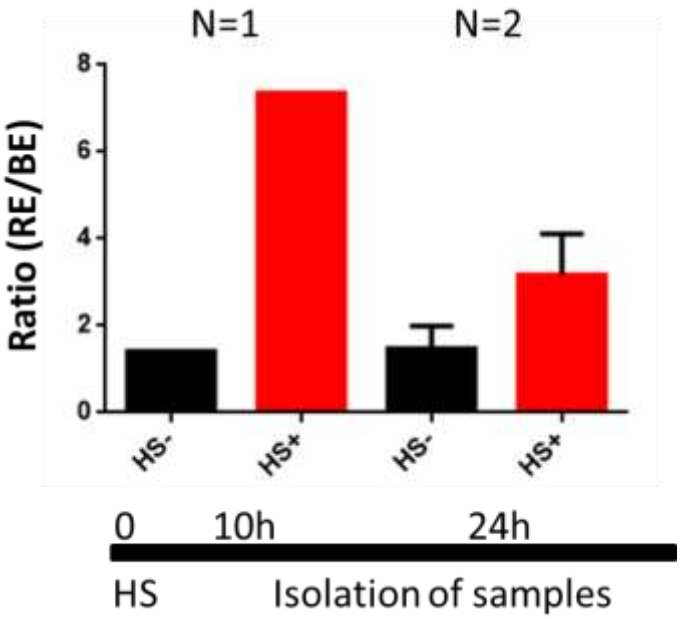


Figure 29.RT-qPCR for *cnfn* induction in transgenic animals. At zero hour, we induced the expression of the transgene by a single heat shock and 10 and 24 hours later we isolated the spinal cord samples to RNA extraction and subsequent RT-qPCR. The ratio compares the red eyes (RE) induction with the black eyes animals (BE) which does not carry the transgene.

*4.1.5.2 Qualitative and Quantitative analysis*

We performed three independent functional assays to study the effects of cnfn overexpression after spinal cord injury. For this, we did qualitative and quantitative assays. The qualitative assays determine the response of the tadpole to a non-aversive stimulus (Figure 30) (Gaete et al., 2012). The quantitative assays determine the total distance swam by the tadpole in 5 minutes (Figure 31) (Muñoz et al., 2015). Since there was not interference between these two assays, we used the same set of animals for both tests.

For comparisons we used the RE animals as controls. We did not find differences between the groups in any of the days tested and in any behavioral analysis (Figure 32 and 33).

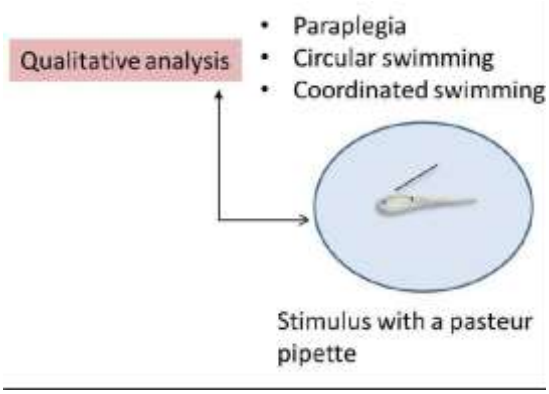


Figure 30. Work scheme of the qualitative analysis performed on the recorded days. Before the 5 minutes of habituation for the recording of the video, we made a soft stimulus in the head skin with a Pasteur pipette. The aversive response is noted (Paraplegia, circular swimming, and coordinated swimming).

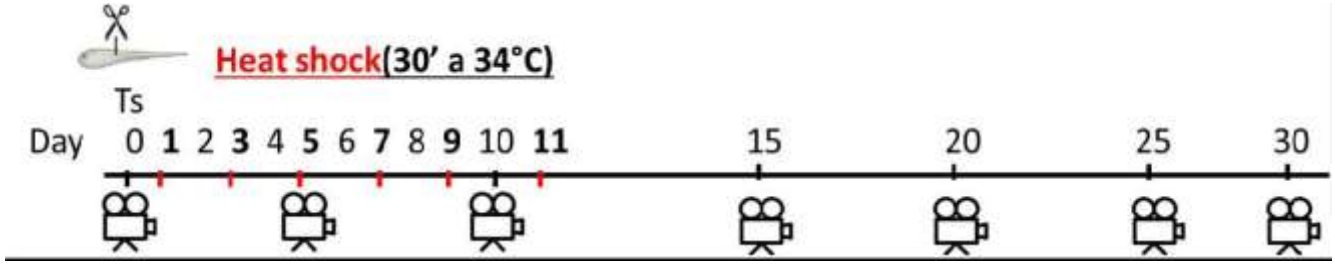


Figure 31. Work scheme for the functional assays. The red lines represent the days in which the animals were exposed to heat shock (30 minutes at 34°C). The cameras represent the days when we recorded the swimming ability of these animals. Ts: transection.

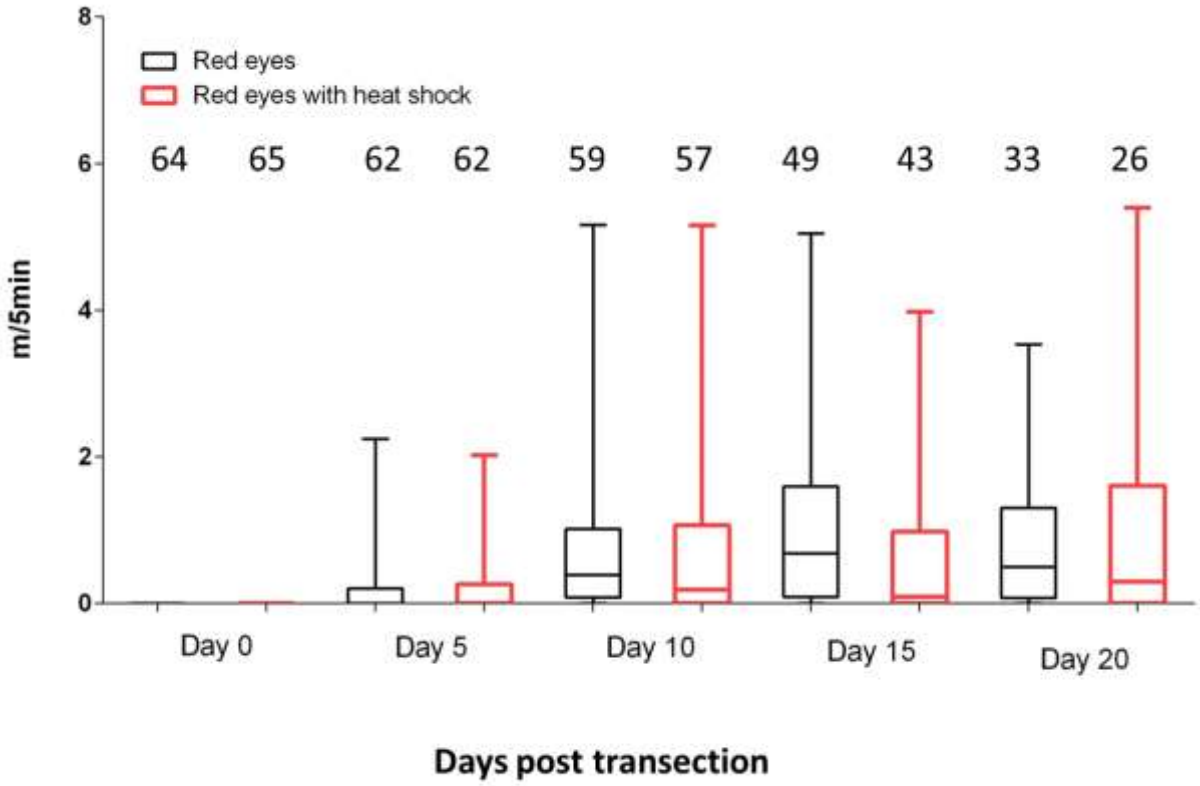


Figure 32. Quantitative analysis. Distances traveled by tadpoles in five minutes of swimming assay graphed in box and whisker plot. The animals of each group are recorded every five days until day 20. The number above each data represents the total number of animals used for this study in every recorded day.

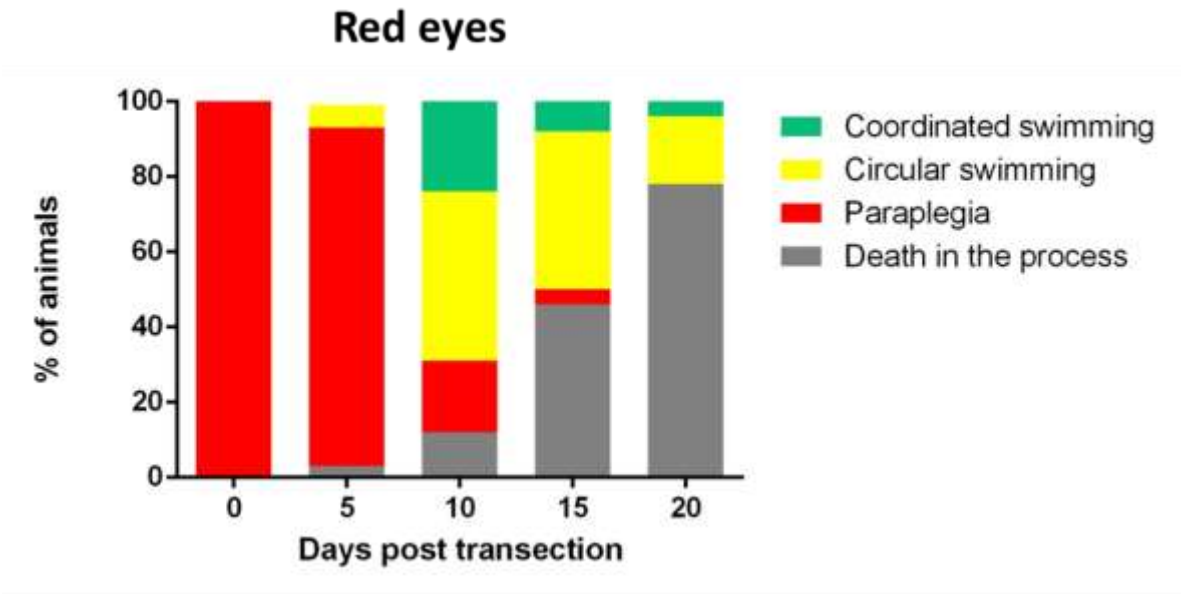


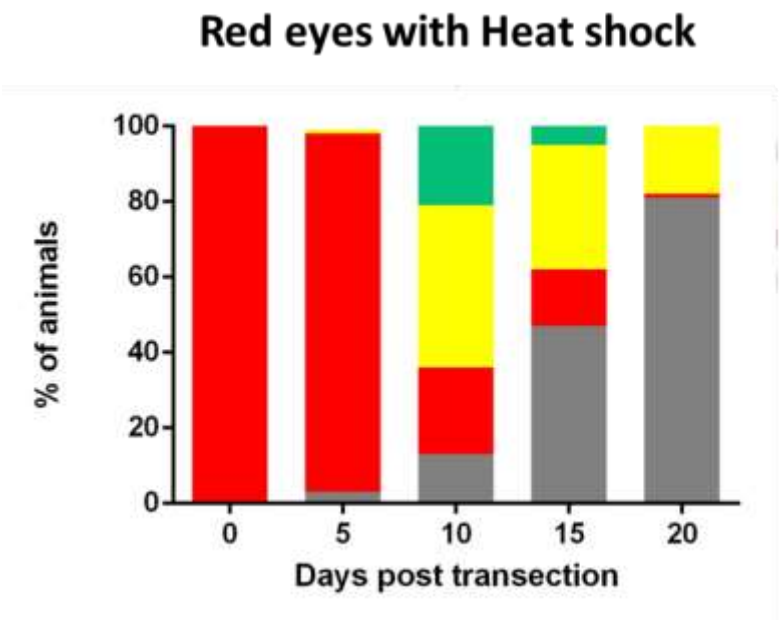


Figure 33. Qualitative analysis. Response to a stimulus are shown in percentage for each studied day (every five days since day 0). In red is paraplegia, in yellow circular swimming, and in green, coordinated swimming. The grey represents the accumulated death percentage of tadpoles during the process.

*4.1.5.3 Protein expression of the transgenic animals after heat shock*

To understand further these results, we isolated spinal cords of BE, RE, and RE+HS animals after 10 and 24 hours after a single heat shock. We detected three set of bands, one between 10 and 15 KDa, one at 15 KDa, and the third one at between 15 and 25 KDa, as we observed in chapter 1. After 10 hours, we did not detect any difference in the protein expression of cnfn, but after 24 hours the levels of the RE+ HS group decreased (Figure 34 lane 3), similar to what we observed on the mRNA levels. Importantly, the overexpression of cnfn was not detected. We kept exploring this discrepancy and performed protein analysis with 2A and GFP antibodies for test these same samples (Figure 35a and 35b). For both antibodies tested, the detected bands did not fall into theoretical expected weights (2 KDa for antibody 2A and 27 KDa to GFP). With the 2A antibody, the bands fell between 35 and 55 KDa and with GFP antibody at 15 KDa. GFP-antibody detected a band also on control animals, which did not carry the transgene, suggesting an unspecific reaction.

Finally, we sequenced the construct of RE transgenic animal to analyze the transgene with Sp6 and T7 promoters. The sequence detected (Figure 35 and 36) is the same as was designed and there were not overlaps or gaps in the sequences inside the construct. Hence, the construct is correct.

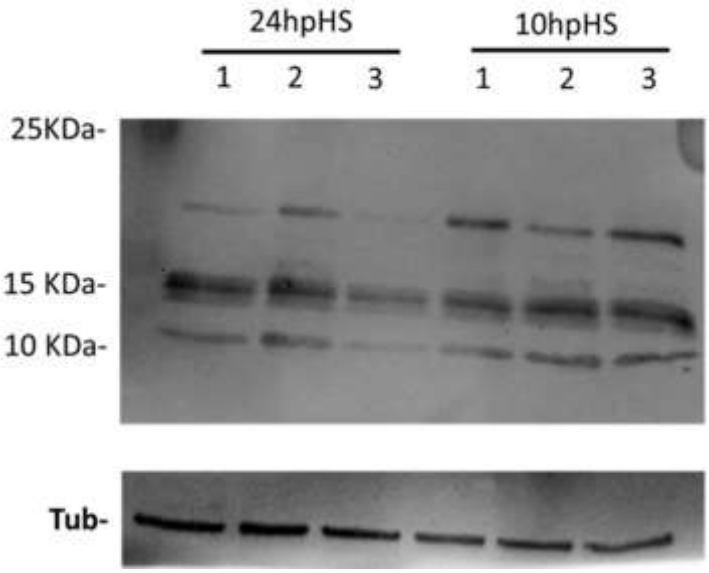


Figure 34. Western blot for cnfn (1:5000; 15 KDa) on spinal cord samples from transgenic animals after 24 and 10 hours of one heat shock induction. Tubulin (1:40000) was used as loading control. Lane 1: Black eyes animals. Lane 2: Red eye animals. Lane 3: Red eyes animals with heat shock. hpHS: Hours post heat shock.

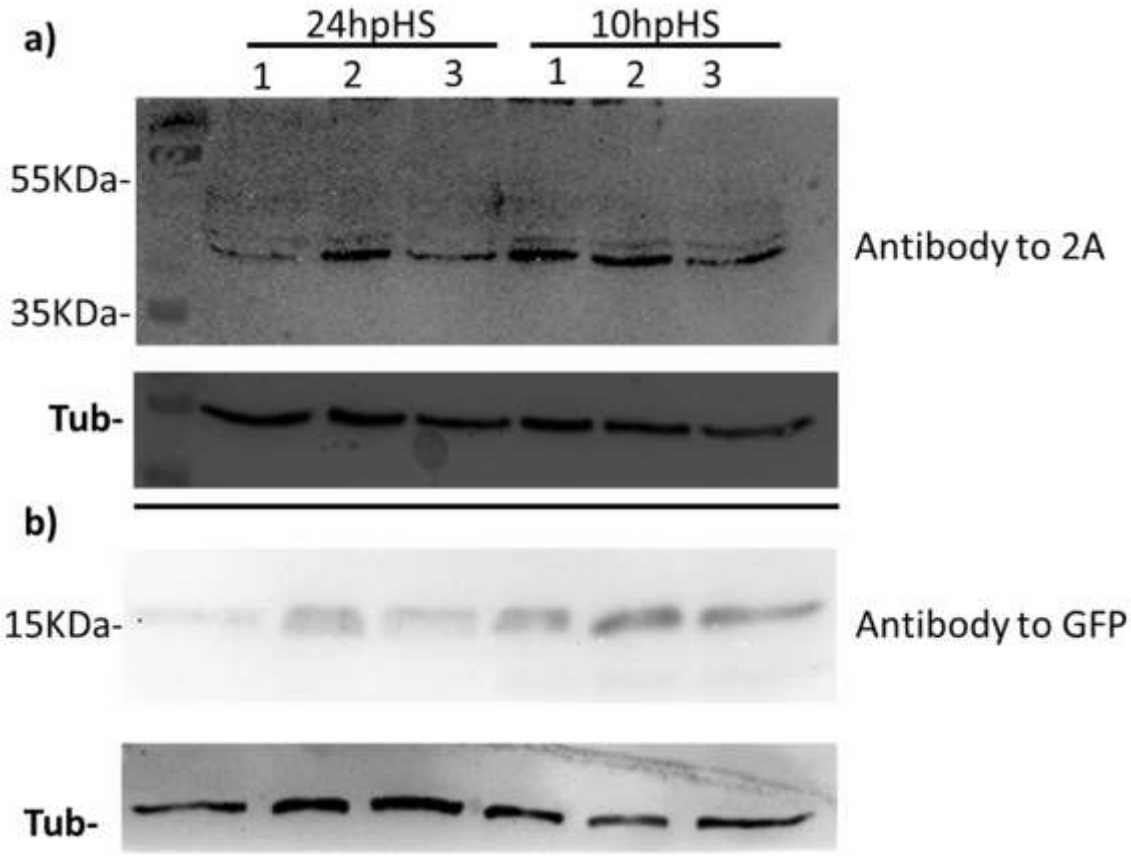


Figure 35. Western blot of the transgenic samples for 2A (1:1000) and GFP-antibody (1:1000) after 24 and 10 hours of one heat shock induction. Tubulin is used as a loading control (1:40000). Lane 1: Black eyes animals. Lane 2: Red eyes animals. Lane 3: Red eyes animals with heat shock.


Figure 36. Reconstruction of the sequenced transgenic animal from Sp6 side.

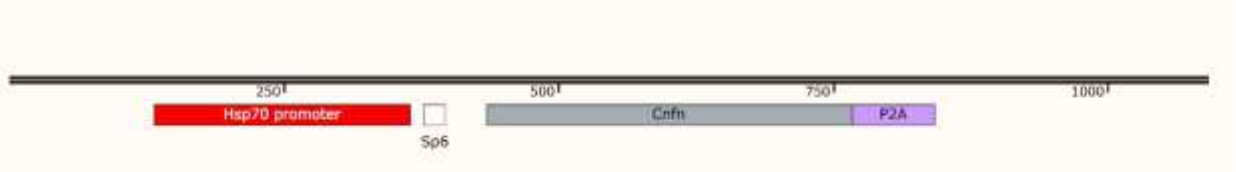


Figure 37. Reconstruction of the sequenced transgenic animal from T7 side.

# 5 DISCUSSION

## *5.1 Cornifelin expression on Xenopus laevis*

In this work, we described the expression of cnfn in the spinal cord and the eye of *Xenopus laevis* during metamorphosis and in response to spinal cord injury. We detected cnfn on the grey matter and meninges from the spinal cord, several layers of the retina, and in the cornea. After injury by transection, cnfn expression was upregulated on NR-animals. We also found striking participation of cnfn on meninges one day after the injury on R-animals and after ten days on NR-animals.

In parallel, we studied the reaction of meningeal cells after the injury with histological techniques such as Masson to detect collagen I and Hematoxylin & Eosin to describe the tissue. On R-animals, an increase in the thickness of the leptomeninges was observed, but no deposition of collagen fibers was found. On the other side, on NR-animals, leptomeningeal layers enclose the stumps, in line with our cnfn expression results on day 10. Collagen fibers were detected on day 20 after the injury. This deposition was found in the injury gap associated with cell groups resembling a rosette-like structure.

Finally, we tested a transgenic line to overexpress cnfn. The behavioral experiments did not find differences between the control and the treated group. When we studied the mRNA levels after one heat shock to overexpress cnfn, we detected an increase of 5 times ten hours after the induction and two times after 24 hours. But on western blot experiments, we did not detect an increase in cnfn expression.

We used several methods to characterize *Xenopus laevis* cnfn, gaining more insight into this poorly studied protein.

On RT-qPCR assays, we found a high variability between different batches of animals of the same stage, overall on pre-metamorphic stages on the spinal cord (NF 50-54). On the contrary, in the eye, we found a high variability on NF-58. During metamorphosis, these issues have also been reported for animals and vary among different genes. The variability of the gene expression during uninjured conditions could account for the results obtained on protein experiments in which the variability between biological replicates surpasses a tendency. First, we use wild-type animals for our studies, so we usually have some variability between the replicates. Besides, it is possible that these high variations in cnfn levels could also be explained by processes occurring on these stages on the tissues studied. During NF-50 and 54, there is still a high proliferation rate on the spinal cord. At the end of this later stage, the differentiation process occurs on neural cells ( Thors, Kort, & Nieuwenhuys, 1982), suggesting a context with many internal changes. Likewise, in the development of the retina and cornea, several changes occur during metamorphic stages. Even though the retina is a fully differentiated structure in early developmental stages, the remodeling of the photoreceptors is frequent (Kevany & Palczewski, 2010). On the other side, there is an increase in epithelial cell death on the cornea during stages 55 and 60, leading to the tissue's remodeling and maturation (Hu et al., 2013). The mRNA variability observed on stage 58 biological replicates could be explained by these factors.

Nevertheless, this problem could be resolved by augmenting the number of biological replicates to decrease their variation. For experiments of this type in the laboratory, three to

four biological replicates are needed to obtain an effect size of 0.8. Still, the number of replicates depends on the gene or protein analyzed and the stage being studied.

We referred to the literature on protein experiments to find tissues helpful as positive controls. We found that the homogenized back skin and eye had the highest abundance of protein with bands close to the theoretical weight of cnfn. The spinal cord from stage 50 animals had the lowest expression in comparison. This may explain the difficulties during the protein experiments on spinal cord tissue development, which we did not have with eye samples. However, the antibody gave a consistent immunoreactivity pattern on the tissues studied and correlated with our In situ hybridization results. We found that neurons from the gray matter were positive to cnfn. This expression had a gradient from medial cells, the ones closest to the central canal, with weaker labeling; and increasing at lateral regions. During mammalian spinal cord development, neuroblasts originate from neural progenitors in the ependymal cell layers and then migrate outwards (Caspary & Anderson, 2003; Helms & Johnson, 2003; Lu, Niu, & Alaynick, 2015). If the same happens in *Xenopus* NF-50, our results would be suggesting that neurons with a higher degree of differentiation present higher protein levels. Moreover, this expression seems to be conserved since cnfn is also found in the neurons of the murine spinal cord at 4 and 56 days, with a more robust mRNA expression on adult tissue (Allen Reference Atlas – MouseSpianl.Brain [spinal atlas]. Available from atlas.brain-map.org).

In contrast, we did not detect this pattern in later stages, NF-58 and 66. The neurons labeled had a homogenous but weaker intensity. Moreover, in NF-66, a rostro-caudal gradient was present with weaker immunoreactivity in rostral sections. The labeling was more evident in

motor neurons, probably due to its size. We also found positive labeling in cells from the central canal. These cells are organized like a pseudo-stratified epithelium from NF-50 to 66 (Edwards-Faret et al., 2018). In NF-50, the expression was restricted to ventral cells and had a rostro-caudal gradient. This result goes in line with previous work from our laboratory that suggests that cells from the dorsal central canal are the ones that proliferate after injury (Edwards-Faret et al., 2021). Cnfn is thus restricted to non-proliferative cells within the central canal of the spinal cord.

To understand the role of cnfn during the regeneration of the *Xenopus laevis* spinal cord, we used a transgenic line that overexpresses cnfn after heat shock induction. After we settled the work schedule (Figure 30 and 31), we began analyzing the cnfn mRNA behavior after the heat shock and began our functional studies. The construct used had the protein tdTomato fused with the gamma-crystallin promoter, the complete cnfn *Xenopus* sequence under the heat shock 70 protein, and the 2A peptide along with the GFP protein. The animals were selected due to the presence or absence of the red crystalline under a fluorescence lamp. Likewise, due to the design of the construct, we were going to be able to see if the induction occurred observing the animal under a fluorescent lamp because of the GFP being released. We were able to see the red eye of the animals that carry the construct but not the green color after heat shock. We did detect changes on the mRNA behavior after heat shock induction. In comparing the groups with their control pairs, we found a fourfold increase on the animals carrying the construct after ten hours. This overexpression diminished after 24 hours, indicating a quick induction and a quick degradation/utilization of the mRNA, which may be related to its stability.

The quantitative and qualitative experiments were carried out before the arrival of the antibody. Three biological replicates were used. The results showed no differences between the control and treated groups suggesting that the overexpression of the cnfn mRNA detected did not affect the regeneration process of these animals.

According to the protein results, after 10 hours of induction by heat shock, there is no difference in expression levels between animals without the transgene (scenario: basal cnfn), the animals that carry the transgene but were not induced (scenario: basal cnfn), and the animals that have the transgene and were induced (scenario: basal cnfn + overexpressed cnfn), indicating that at ten hours the mRNA is not being translated. Moreover, at 24 hours of induction, a reduction in the expression of cnfn is observed for animals with the transgene induced. We did not detect any overexpression on the protein levels of cnfn. We performed western blot for peptide 2A and GFP to gain insight into this discrepancy. Both results show bands with weights that differ significantly from those expected. Although we detected bands with the GFP antibody on control animals that did not carry the transgene suggesting an unspecific union, we have other clues that guide us to think that the transgene did not cleave and thus did not release cnfn after the heat shock; this way we do not detect its overexpression. First, we did not observe any green animals after the heat shock induction; therefore, the GFP was not released. Second, we did not detect the overexpression of the cnfn protein on transgenic animals after the induction. Third, the antibody to 2A, used previously by other laboratory members with expected results, detected bands that fall between 35 and 55 KDa. This result makes us suspect that we detected the entire transgene, as the sum of cnfn+2A+GFP is 12+2+27=41 KDa approximately. Fourth, we sequenced the

construct from a RE animal and found no gaps or overlaps. This construct contains a promoter, used with success in other lines of the laboratory (Faunes, et al, 2017), a site of transcription initiation, a site of polyadenylation, and a site of transcription termination (Chaible, et al.,2013).

The bands obtained by the cnfn antibody correspond to endogen proteins, indicating that although mRNAs are expressed after heat shock, they are not translated. Thus the transgenic line does not overexpress the cnfn protein.

*5.3 Cnfn is expressed in squamous-like tissues*

In our results, we detected the expression of cnfn on two structures that had a high turnover rate, the outer segment of the photoreceptors and the corneal epithelium of *Xenopus laevis*. These two structures are constantly renewing as part of their homeostatic process and in response to injury. Like the skin, the corneal epithelia act as a physical barrier protecting the eye from external cues. The NF-50 *Xenopus* cornea is still in development. The corneal epithelium is a stratified structure formed by squamous cells (Dhouailly et al., 2014) that consists of an inner layer of endothelial tissue, a stroma layer in the middle whose cells are in division; and the outer cornea formed by keratocytes, that begins accumulating collagen fibers (Hu, 2013). On the other side, although not a squamous epithelium, the retinal outer segment is subjected to a similar process; it renews by shedding the most distal parts of the photoreceptors disks. Then, the shed material is phagocyted by RPE cells (Kevany B.M, 2010). Therefore, our results agree with previous studies that describe cnfn in epithelia that renew by shedding (Human Protein Atlas available from http://www.proteinatlas.org, v20.1; Uhlen et al., 2010).

*5.4 Cnfn would be a player of the wound healing process after injury*

Tissue lesions trigger a wound closure reaction. The wound healing process encompasses hemostasis, inflammation, repair, and remodeling (Moretti, et al., 2022).

On a microarray work studying **limb regeneration and wound healing after arm amputation** in *Xenopus* animals from NF-53 and 57, cnfn was downregulated when they compared the transcripts five days after the amputation (Grow M, 2006), suggesting that cnfn is detrimental for regeneration on regenerative stages. The Gene Ontology (GO) analysis of the gene list downregulated in this work matched with "epithelial development" and "cell differentiation" categories. Cnfn was found in this list along with some other skin proteins like filaggrin, envoplakin, corneodesmosin, caspase-14, cadherin, involucrin, and several keratins. All these genes participate in epithelial homeostasis. These processes occur during development and in response to injury. Both on uninjured and injured epithelia, the cells have to be subjected to cell death, migration, adhesion, and terminal differentiation to maintain the barrier function (Gagliardi & Primo, 2019). On a stratified squamous epithelium like the epidermis, these genes are related to the process of cornification, the death of epidermal cells. Several proteins allow the migration of new cells from the basal membrane to upper layers, the formation of a new cornified envelope, and the desquamation of the stratum corneum to re-establish the barrier (Candi, 2005). Keratins 5 and 14 are part of the proliferation of keratinocytes and their migration to upper layers. On the granular layer, filaggrin participates in the formation of keratins bundles that produce the collapse of the new cells to form the flat cells forming the stratum corneum. Envoplakin is part of the adhesion complexes expressed between the granular and the cornified layer. Caspase-14 is

part of the terminal keratinocyte differentiation, degrading corneodesmosomes to allow the desquamation of the cornified layer (Candi E, 2005).

Cnfn has been implied in a context of accelerated wound healing too, as psoriasis. Cnfn is highly expressed in the epidermis of patients with psoriasis (Michibata H, 2004), an autoimmune skin disease characterized by hyperproliferation and desquamation of the epidermis (Morhenn, 2018). Cnfn is also involved in the desquamation process. In the absence of cnfn there is a decrease in the corneodesmosin expression resulting in the detachment of the cells (Wagner et al, 2019), suggesting a high regulation of cnfn during different stages of psoriasis.

On the other side, the analysis of the gene list from day six in Lee-Liu's work (Lee-Liu et al., 2014), which compares the transcripts from regenerative and non-regenerative animals after **spinal cord injury**, found an enrichment on apoptosis, epithelial to mesenchymal transition, and adherens junction. On this day on NF-66 animals, cnfn is upregulated. We could relate these processes with the wound healing occurring on the spinal cord of NF-66 animals after transection injury that ended up with a scar formation.

Fibroblast cells from the meninges participate in the wound healing process after an injury that compromises the barrier function on the central nervous system. In non-regenerative organisms, there is an increase in the proliferation of these layers, a migration to the injury site, and the re-establishment of the barrier that ends the formation of a fibrotic scar (Decimo I, 2011; Derk J, 2021). On NF-50, fibronectin expression is detected on the cord stumps six days after transection injury and on NF-66, ten days after the injury (Edwards-Faret, 2021). Likewise, our results detected an increase in the cellular infiltration positive to cnfn at one

day after transection injury in NF-50 animals (Figure 22a). This expression was concentrated on the injury gap and the meninges sealing the stumps. The expression and the cellular infiltration tend to clear out as days go by, and the neural tissue reconnects, returning to meninges at day ten. We also observe this behavior with our Masson stain results (Figure 24), showing an increase in the thickness of the leptomeninges that tends to decrease ten days after the injury. But, unlike what happens in non-regenerative animals, in the case of NF-50 animals, regeneration overcomes the wound healing process after an injury, and no fibrotic scar is formed. In this case, and as Zukor described in 2011 for newts, one day after the injury, cells that are continuous with the meninges enclose the caudal stump and open afterward to follow the reconnection of the axons (Zukor et al., 2011).

On the other hand, six days after the injury in NF-66 animals, we started to see some cellular deposition, and on day ten, we found cnfn on the meninges closest to the stumps and the injury gap (Figure 23i). In our Masson stain results, we found an increase in cellular infiltration and the thickness of the meningeal layers. Hematoxylin & Eosin results found meningeal fibers on the gap two days after the injury. At twenty days after the injury, some of the infiltrations have cleared out, and we detect collagen I on the gap, associated with rosette-like cell groups, suggesting a barrier to the reconnection of the central canal.

This differential response in NF-50 versus NF-66 stages proposes an opposite role for cnfn in the reaction after spinal cord injury. The observed expression suggests that meningeal cornifelin positive cells participate in the spinal cord gap sealing in NF-50, while in NF-66 in the generation of the fibrotic scar.

Our results show that cornifelin is expressed during the meningeal re-establishment of the barrier that covers and protects the neural tissue, which must be restored after the injury to restrain secondary damage. Further studies will be required to confirm this hypothesis.

# 6. CONCLUSIONS

1. Cnfn is expressed on the grey matter and meninges of the spinal cord of *Xenopus laevis* from NF-50 to 66.

2. Both the expression of the mRNA and the protein on the spinal cord decrease during metamorphosis.

3. Cnfn is expressed on the ganglion cell layer, on the inner and outer nuclear layer, and the outer segment of the retina *Xenopus laevis* from NF-50 to 66.

4. Cnfn is expressed on the outer cornea and the stroma of the cornea from NF-50 animals.

5. There is a change in the location of cnfn immunoreactivity on the photoreceptor layer from the cell body to the membrane of the outer segment.

6. Cnfn expression on the spinal cord changes after injury, it is downregulated at NF-50 and downregulated at NF-66.

7. Cnfn participates on the meningeal reaction to injury.

# 7. BIBLIOGRAPHY


Achtstatter, T., Fouquet, B., & Franke, W. W. (1989). *Differentiat ion Cytokeratin filaments and desmosomes in the epithelioid cells of the perineurial and arachnoidal sheaths of some vertebrate species*. 129–149.

Aldea, D., Hanna, P., Munoz, D., Espinoza, J., Torrejon, M., Sachs, L., … Marcellini, S. (2013). *Evolution of the Vertebrate Bone Matrix : An Expression Analysis of the Network Forming Collagen Paralogues in Amphibian Osteoblasts*. 375–384. https://doi.org/10.1002/jez.b.22511

Alizadeh, A., Dyck, S. M., & Karimi-abdolrezaee, S. (2019). *Traumatic Spinal Cord Injury : An Overview of Pathophysiology , Models and Acute Injury Mechanisms*. *10*(March), 1–25. https://doi.org/10.3389/fneur.2019.00282

Anderson, M. A., Burda, J. E., Ren, Y., Ao, Y., Shea, T. M. O., Kawaguchi, R., … Michael, V. (2016). Astrocyte scar formation aids central nervous system axon regeneration. *Nature*, *532*(7598), 195–200. https://doi.org/10.1038/nature17623

Becker, C. G., Becker, T., & Hugnot, J. P. (2018). The spinal ependymal zone as a source of endogenous repair cells across vertebrates. *Progress in Neurobiology*, *170*(January), 67–80. https://doi.org/10.1016/j.pneurobio.2018.04.002

Bradbury, E. J., & Carter, L. M. (2011). Manipulating the glial scar : Chondroitinase ABC as a therapy for spinal cord injury. *Brain Research Bulletin*, *84*(4–5), 306–316. https://doi.org/10.1016/j.brainresbull.2010.06.015

Cabreira-Cagliari, C., Dias, N. D. C., Bohn, B., Fagundes, D. G. D. S., Margis-Pinheiro, M., Bodanese-Zanettini, M. H., & Cagliari, A. (2018). Revising the PLAC8 gene family: From a central role in differentiation, proliferation, and apoptosis in mammals to a multifunctional role in plants. *Genome*, *61*(12), 857–865. https://doi.org/10.1139/gen-2018-0035

Candi, E., Schmidt, R., & Melino, G. (2005). *THE CORNIFIED ENVELOPE : A MODEL OF CELL DEATH IN THE SKIN*. *6*(April). https://doi.org/10.1038/nrm1619

Caspary, T., & Anderson, K. V. (2003). Patterning cell types in the dorsal spinal cord: What the mouse mutants say. *Nature Reviews Neuroscience*, *4*(4), 290–298. https://doi.org/10.1038/nrn1073

Chaible, L. M., Kinoshita, D., Corat, M. A. F., & Zaidan, M. L. (2013). Genetically Modified Animal Models. In *Animal Models for the Study of Human Disease*. https://doi.org/10.1016/B978-0-12-415894-8.00033-6

Choi, S., Lee, M., Lee, S. H., Jung, H. S., Kim, S. Y., Chung, T. Y., … Lim, K. M. (2014). Identification of cornifelin and early growth response-1 gene as novel biomarkers for in vitro eye irritation using a 3D reconstructed human cornea model MCTT HCE??? *Archives of Toxicology*, *89*(9), 1589–1598. https://doi.org/10.1007/s00204-014-1390-8

Decimo, I. (2011). Nestin- and Doublecortin-Positive Cells Reside in Adult Spinal Cord Meninges and Participate in Injury-Induced Parenchymal Reaction. *Stem Cell*, *29*, 2062–2076. https://doi.org/10.1002/stem.766

Derk, J., Jones, H. E., Como, C., Pawlikowski, B., Siegenthaler, J. A., & Gilli, F. (2021).

*Living on the Edge of the CNS : Meninges Cell Diversity in Health and Disease*. *15*(July). https://doi.org/10.3389/fncel.2021.703944

Duncan, I. D., Aguayo, A. J., Bunge, R. P., & Wood, P. M. (1981). Transplantation of rat schwann cells grown in tissue culture into the mouse spinal cord. *Journal of the Neurological Sciences*, *49*(2), 241–252. https://doi.org/10.1016/0022-510X(81)90082-4

Edwards-faret, G., Muñoz, R., Méndez-olivos, E. E., Lee-liu, D., Tapia, V. S., & Larraín, J. (2017). Spinal cord regeneration in Xenopus laevis. *Nature Publishing Group*, *12*(2), 372–389. https://doi.org/10.1038/nprot.2016.177

Faunes, F., Gundermann, D. G., Muñoz, R., Bruno, R., & Larraín, J. (2017). The heterochronic gene Lin28 regulates amphibian metamorphosis through disturbance of thyroid hormone function. *Developmental Biology*, (March), 0–1. https://doi.org/10.1016/j.ydbio.2017.03.026

Fei, J. F., Schuez, M., Tazaki, A., Taniguchi, Y., Roensch, K., & Tanaka, E. M. (2014). CRISPR-mediated genomic deletion of Sox2 in the axolotl shows a requirement in spinal cord neural stem cell amplification during tail regeneration. *Stem Cell Reports*, *3*(3), 444–459. https://doi.org/10.1016/j.stemcr.2014.06.018

Gaete, M., Muñoz, R., Sánchez, N., Tampe, R., Moreno, M., Contreras, E. G., … Larraín, J. (2012). *Spinal cord regeneration in Xenopus tadpoles proceeds through activation of Sox2-positive cells*. 1–17.

Gagliardi, P. A., & Primo, L. (2019). Death for life : a path from apoptotic signaling to tissue - scale effects of apoptotic epithelial extrusion. *Cellular and Molecular Life Sciences*, *76*(18), 3571–3581. https://doi.org/10.1007/s00018-019-03153-x

Grine, L., Dejager, L., Libert, C., & Vandenbroucke, R. E. (2015). Dual Inhibition of TNFR1 and IFNAR1 in Imiquimod-Induced Psoriasiform Skin Inflammation in Mice. *The Journal of Immunology*, *194*(11), 5094–5102. https://doi.org/10.4049/jimmunol.1403015

Guo, Y., Ma, L., Cristofanilli, M., Hart, R. P., Hao, A., & Schachner, M. (2011). Transcription factor Sox11b is involved in spinal cord regeneration in adult zebrafish. *Neuroscience*, *172*, 329–341. https://doi.org/10.1016/j.neuroscience.2010.10.026

He, Z., & Jin, Y. (2016). Review Intrinsic Control of Axon Regeneration. *Neuron*, *90*(3), 437–451. https://doi.org/10.1016/j.neuron.2016.04.022

Helms, A. W., & Johnson, J. E. (2003). Specification of dorsal spinal cord interneurons. *Current Opinion in Neurobiology*, *13*(1), 42–49. https://doi.org/10.1016/S0959-4388(03)00010-2

Hu, W., Haamedi, N., Lee, J., Kinoshita, T., & Ohnuma, S. ichi. (2013). The structure and development of Xenopus laevis cornea. *Experimental Eye Research*, *116*, 109–128. https://doi.org/10.1016/j.exer.2013.07.021

J, F. (1995). Spinal axons in central nervous system scar tissue are closely related to laminin-immunoreactive astrocytes. *Neuroscience*, *65*(1), 293–304.

Kevany, B. M., & Palczewski, K. (2010). Phagocytosis of retinal rod and cone photoreceptors. *Physiology*, *25*(1), 8–15. https://doi.org/10.1152/physiol.00038.2009

Lee-liu, D., Moreno, M., Almonacid, L. I., Tapia, V. S., Muñoz, R., Marées, J. Von, … Larraín, J. (2014). *Genome-wide expression profile of the response to spinal cord injury in Xenopus laevis reveals extensive differences between regenerative and non-regenerative stages*. 1–20.

Liu, K.-M., Chen, Y.-J., Shen, L.-F., Haddad, A. N. S., Song, I.-W., Chen, L.-Y., … Chen, Y.-T. (2015). Cyclic alopecia and abnormal epidermal cornification in Zdhhc13-deficient mice reveal the importance of palmitoylation in hair and skin differentiation. *Journal of Investigative Dermatology*, *135*(11), 2603–2610. https://doi.org/10.1038/jid.2015.240

Lu, D. C., Niu, T., & Alaynick, W. A. (2015). Molecular and cellular development of spinal cord locomotor circuitry. *Frontiers in Molecular Neuroscience*, *8*(June), 1–18. https://doi.org/10.3389/fnmol.2015.00025

Méndez-Olivos, E. E., Muñoz, R., & Larraín, J. (2017). Spinal Cord Cells from Pre-metamorphic Stages Differentiate into Neurons and Promote Axon Growth and Regeneration after Transplantation into the Injured Spinal Cord of Non-regenerative Xenopus laevis Froglets. *Frontiers in Cellular Neuroscience*, *11*(December), 1–15. https://doi.org/10.3389/fncel.2017.00398

Michibata, H., Chiba, H., Wakimoto, K., Seishima, M., Kawasaki, S., Okubo, K., … Imai, Y. (2004). *Identification and characterization of a novel component of the cornified envelope, cornifelin*. *318*, 803–813. https://doi.org/10.1016/j.bbrc.2004.04.109

Mokalled, M. H., Patra, C., Dickson, A. L., Endo, T., Stainier, D. Y. R., & Poss, K. D. (2016). Injury-induced <em>ctgfa</em> directs glial bridging and spinal cord regeneration in zebrafish. *Science*, *354*(6312), 630 LP – 634. https://doi.org/10.1126/science.aaf2679

Moretti, L., Stalfort, J., Barker, T. H., & Abebayehu, D. (2022). The interplay of fibroblasts, the extracellular matrix, and inflammation in scar formation. *Journal of Biological Chemistry*, 101530. https://doi.org/10.1016/j.jbc.2021.101530

Morhenn, V. B. (2018). *The Relationship of Wound Healing with Psoriasis and Multiple Sclerosis*. *7*(6), 185–188. https://doi.org/10.1089/wound.2017.0773

Morphogenesis, I., Thors, F., Kort, E. J. M. De, & Nieuwenhuys, R. (1982). *Anatomy and Embryology On the Development of the Spinal Cord of the Clawed Frog , Xenopus laevis*. 427–441.

Morse, D. E., & Low, F. N. (1972). The fine structure of the pia mater of the rat. *American Journal of Anatomy*, *133*(3), 349–367. https://doi.org/10.1002/aja.1001330309

Muñoz, R., Edwards-faret, G., Moreno, M., Zuñiga, N., Cline, H., & Larraín, J. (2015). *Regeneration of Xenopus laevis spinal cord requires Sox2 / 3 expressing cells*. https://doi.org/10.1016/j.ydbio.2015.03.009

Nicholas, D. S., & Roy, O. (1988). *The fine anatomy of the human spinal meninges*. *69*, 276–282.

Ogai, K., Nakatani, K., Hisano, S., Sugitani, K., Koriyama, Y., & Kato, S. (2014). Function of Sox2 in ependymal cells of lesioned spinal cords in adult zebrafish. *Neuroscience Research*, *88*, 84–87. https://doi.org/10.1016/j.neures.2014.07.010

Pekny, M., Pekna, M., Messing, A., Steinhäuser, C., Moo, J., Vladimir, L., … Verkhratsky, A. (2016). Astrocytes : a central element in neurological diseases. *Acta Neuropathologica*, *131*(3), 323–345. https://doi.org/10.1007/s00401-015-1513-1

Sabelström, H., Stenudd, M., Réu, P., Dias, D. O., Elfineh, M., Zdunek, S., … Frisén, J. (2013). *After Spinal Cord Injury in Mice*. *537*(November), 534–537.

Silver, J., & Miller, J. H. (2004). *REGENERATION BEYOND THE GLIAL SCAR*. *5*(February), 146–156. https://doi.org/10.1038/nrn1326

Silver, J., Schwab, M. E., & Popovich, P. G. (2015). Central Nervous System Regenerative Failure : *Cold Spring Harb Perspect Biol*, *7*, a020602. https://doi.org/10.1101/cshperspect.a020602

Song, W. Y., Hörtensteiner, S., Tomioka, R., Lee, Y., & Martinoia, E. (2011). Common functions or only phylogenetically related? The large family of PLAC8 motif-containing/PCR genes. *Molecules and Cells*, *31*(1), 1–7. https://doi.org/10.1007/s10059-011-0024-8

Suter, T. A. C. S., DeLoughery, Z. J., & Jaworski, A. (2017). Meninges-derived cues control axon guidance. *Developmental Biology*. https://doi.org/10.1016/j.ydbio.2017.08.005

Thierry-Mieg, D., & Thierry-Mieg, J. (2006). AceView: a comprehensive cDNA-supported gene and transcripts annotation. *Genome Biology*, *7 Suppl 1*(Suppl 1), 1–14. https://doi.org/10.1186/gb-2006-7-s1-s12

Uhlen M, 2010. (2010). *Towards a knowledge-based Human Protein Atlas*. *28*(12), 12–14. https://doi.org/10.1038/nbt1210-1248

Wagner, T., Beer, L., Gschwandtner, M., Eckhart, L., Kalinina, P., Laggner, M., … Mildner, M. (2019). The Differentiation-Associated Keratinocyte Protein Cornifelin Contributes to Cell-Cell Adhesion of Epidermal and Mucosal Keratinocytes. *Journal of Investigative Dermatology*, *139*(11), 2292-2301.e9. https://doi.org/10.1016/j.jid.2019.04.019

Wang, T., Zhou, Z., Luo, E., Zhong, J., Zhao, D., Dong, H., & Yao, B. (2021). Comprehensive RNA sequencing in primary murine keratinocytes and fibroblasts identifies novel biomarkers and provides potential therapeutic targets for skin-related diseases. *Cellular and Molecular Biology Letters*, *26*(1). https://doi.org/10.1186/s11658-021-00285-6

Yan, B., Neilson, K. M., Ranganathan, R., Maynard, T., Streit, A., & Moody, S. A. (2015). *Microarray Identification of Novel Genes Downstream of Six1 , a Critical Factor in Cranial Placode , Somite , and Kidney Development*. 181–210. https://doi.org/10.1002/DVDY.24229

Yuan, Y., & He, C. (2013). *The glial scar in spinal cord injury and repair*. *29*(4), 421–435. https://doi.org/10.1007/s12264-013-1358-3

Zukor, K. A., Kent, D. T., & Odelberg, S. J. (2011). Meningeal cells and glia establish a permissive environment for axon regeneration after spinal cord injury in newts Meningeal cells and glia establish a permissive environment for axon regeneration after spinal cord injury in newts. *Neural Development*, *6*(1), 1. https://doi.org/10.1186/1749-8104-6-1